

## RESEARCH LETTER

# Social context prevents heat hormetic effects against mutagens during fish development

Lauric Feugere<sup>1,\*</sup> , Claudio Silva De Freitas<sup>1</sup>, Adam Bates<sup>1,†</sup>, Kenneth B. Storey<sup>2</sup>, Pedro Beltran-Alvarez<sup>3</sup> and Katharina C. Wollenberg Valero<sup>1,4,5</sup> 

<sup>1</sup> Department of Biological and Marine Sciences, University of Hull, Kingston upon Hull, UK

<sup>2</sup> Department of Biology, Carleton University, Ottawa, Canada

<sup>3</sup> Biomedical Institute for Multimorbidity, Centre for Biomedicine, Hull York Medical School, University of Hull, Kingston upon Hull, UK

<sup>4</sup> School of Biology and Environmental Science, University College Dublin, Ireland

<sup>5</sup> Conway Institute, University College Dublin, Ireland

## Correspondence

K. C. Wollenberg Valero, Department of Biological and Marine Sciences, University of Hull, Cottingham Road, Kingston upon Hull HU6 7RX, UK  
 Tel: +353 1 716 2385  
 E-mail: [katharina.wollenbergvalero@ucd.ie](mailto:katharina.wollenbergvalero@ucd.ie)

## Present address

\*Marine Ecological and Evolutionary Physiology (MEEP) Laboratory, Département de Biologie, Chimie et Géographie, Université du Québec à Rimouski, Canada  
<sup>†</sup>Department of Psychiatry, Warneford Hospital, University of Oxford, UK

(Received 21 March 2025, accepted 28 March 2025)

doi:10.1002/1873-3468.70047

Edited by Claus M. Azzalin

Since stress can be transmitted to congeners *via* social metabolites, it is paramount to understand how the social context of abiotic stress influences aquatic organisms' responses to global changes. Here, we integrated the transcriptomic and phenotypic responses of zebrafish embryos to a UV damage/repair assay following scenarios of heat stress, its social context and their combination. Heat stress preceding UV exposure had a hormetic effect through the cellular stress response and DNA repair, rescuing and/or protecting embryos from UV damage. However, experiencing heat stress within a social context negated this molecular hormetic effect and lowered larval fitness. We discuss the molecular basis of interindividual chemical transmission within animal groups as another layer of complexity to organisms' responses to environmental stressors.

**Keywords:** carryover effect; DNA repair; heat stress; hormetic effect; stress communication; UV damage

In an era of fast-paced climate change, thermal anomalies such as extreme temperatures are becoming more frequent [1,2]. Such heat events may cause sharp declines in fitness in ectotherms [3]. Aquatic

ectotherms, such as zebrafish [4], can spawn in shallow waters where offspring experience high temperatures and environmental mutagens including ultraviolet radiation (UVR) from sunlight [5]. Moreover,

## Abbreviations

[d], effect size; 6-4PPs, 6-4 photoproducts; ANOVA, analysis of variance; C + UV, control condition followed by UVB/UVA damage/repair treatment; C, control condition; CPDs, cyclobutane pyrimidine dimers; DEG, differentially expressed gene; DNA, deoxyribonucleic acid; dpf, days post fertilisation; GO, gene ontology; hpf, hours post fertilisation; HSP, heat shock protein; KEGG, Kyoto Encyclopedia of Genes and Genomes; LFC, log fold-change of gene expression; PC1, first principal component; PCA, principal component analysis; PCR, polymerase chain reaction; PERMANOVA, permutational analysis of variance; RIN, RNA integrity number; RNA, ribonucleic acid; SM + UV, social metabolites followed by UVB/UVA damage/repair treatment.; SM, social metabolites; TS + SM + UV, social metabolites in thermal stress, followed by UVB/UVA damage/repair treatment; TS + SM, social metabolites in thermal stress; TS + UV, thermal stress followed by UVB/UVA damage/repair treatment; TS, thermal stress; UV, ultraviolet; UVA, ultraviolet A (315–400 nm); UVB, ultraviolet B (280–315 nm); UVR, ultraviolet radiation.

heat-stressed aquatic animals may release metabolites altering the biology of conspecifics not directly experiencing heat stress in a mechanism of stress social communication [6,7]. Embryos developing in clutches may consequently show amplified stress responses to heat due to such 'social metabolites'. Therefore, the understanding of the effects of extreme heat stress on vulnerable aquatic animals as well as their perception of risk *via* chemical ecology emerge as two important avenues of research. However, there is little knowledge about the consequences of the social context of such early-life direct stressors when aquatic animals face subsequent environmental challenges. This is particularly relevant as species inhabit increasingly challenging environments with multiple stressors [8]. When interacting, the response of organisms to these combined stressors may be unexpected due to synergism and antagonism [9] as well as hormesis where stress history protects against future challenges [10,11]. Therefore, predicting the fate of aquatic species in future environments requires a better understanding of the social context of their stress history and the mutagenic environments they encounter.

One prominent mutagenic stressor, UVR, is expected to increase towards the end of the century [12] including in aquatic environments that simultaneously become warmer [1,2]. UVR is a pervasive stressor for a multitude of species [13] including fish [14], explaining that it receives increasing attention in studies within ecological contexts considering multiple stressors [15]. Early-life stages developing outside the maternal body are particularly vulnerable to both UVR [5,13,16] and heat stress [17,18]. Since early-life exposure to UVR lowers fitness in later stages [19,20], it becomes paramount to understand the consequences of heat stress and its social context experienced during early development on the ability to persist within mutagenic environments. For instance, past studies found that abiotic stressors, such as high temperatures, combined with UVR can lead to additive, synergistic or antagonistic effects on the biology of fish [14,21,22]. Mechanistically, heat may denature DNA repair proteins [23,24] and lower energy investment towards DNA repair [25]. Such lowered DNA repair capacity may increase DNA damage, which we hypothesise will affect fitness and survival through increased mutation rates. Prior studies mostly investigated heat simultaneous to UVR. However, stressors can have 'latent carry-over' effects persisting once the initial stressor is removed, which is an important yet overlooked avenue of research [26–29]. The effects of UVR combined with higher temperature may be complex and depend on the timing of heat exposure [30]. In this study, we

investigate carry-over effects, which we refer to as 'stress history', when encountering a subsequent mutagenic environment.

In natural environments, both ultraviolet A (UVA, 315–400 nm) and ultraviolet B (UVB, 280–315 nm) filter through the water column and cause molecular damage to lipids, proteins and DNA [5,14,31]. Most DNA damage is attributable to UVB, whilst UVA (along with blue light) activates photorepair mechanisms that directly reverse DNA lesions such as cyclobutane pyrimidine dimers (CPDs) and 6–4 photoproducts (6-4PPs) [31–33]. Other repair mechanisms include nucleotide excision repair to substitute damaged nucleotides [5,31,34], mismatch repair to remove mispaired bases [35] and homologous recombination and nonhomologous end joining to repair double-strand breaks [31,36]. Failure to mount such repair responses to UVR can impair immunity [21,37] and scale up to whole-body damage such as altered behaviour, locomotion, increased malformations, and in turn, mortality [13,14,38]. UVB may also induce inheritable epigenetic changes such as histone modifications, resulting in inherited resistant phenotypes [39,40]. The well-characterised cellular response to UVR can be harnessed to better understand the damage and repair systems following direct heat stress history and the social context of heat stress through means of social metabolites.

Zebrafish (*Danio rerio*), even at embryonic stages, possess a competent repair system, involving genes in all repair pathways, to remove UVB-induced DNA lesions [32,41–43]. Among these, blue light- and UVA-activated photolyases efficiently photorepair CPDs and 6-4PPs formed during UVB exposure, rescuing zebrafish embryos from UVB-induced morphological defects [32,41]. We recently evidenced that both heat stress and the social context of heat stress *via* social metabolites stressed zebrafish embryos [7,44]. We now ask whether heat stress or social metabolites of heat-stressed embryos affect DNA protection or repair capacity in a mutagenic environment, in terms of nucleic acid integrity and differential expression of repair-relevant genes, and, as a result, affect apparent fitness (reaction to the novel stimuli light and touch) at the phenotypic level. In more detail, we hypothesised ( $H_1$ ) that prior stress history exacerbates the negative consequences of mutagenic environments, ( $H_2$ ) mediated by stress history-dependent alterations of the cellular machinery upon UVR, leading to ( $H_3$ ) increased emergence of mutant phenotypes with fitness outcomes more greatly adversely affected by more complex stress history. At the cellular level, we expected stress history to act on the DNA repair

pathway [33], heat shock response (i.e. protein folding) [45], RNA and protein methylation [46,47] and epigenetic gene expression regulation [48] due to their known roles in repairing and protecting macromolecules upon UV exposure.

## Materials and methods

### Zebrafish handling methods

Adult zebrafish (*Danio rerio*, AB strain) stocks were obtained from the Universities of Sheffield and Cambridge and were maintained at the University of Hull in a temperature-controlled room at 27 °C with a 14 : 10 light : dark cycle. Fish were fed twice a day an alternate diet of mini-bloodworm, daphnia and dried flakes. Breeding consisted of placing plastic trays filled with marbles and plastic plants, directly in the adult fish stock tanks, in the afternoon prior, and collecting zebrafish embryos at 10 am. Zebrafish embryos were cleaned in fresh E3 embryo medium [49] and then bleached by immersion for 3 min in each of the following baths: (a) bleaching medium, (b) embryo medium, (c) bleaching medium, (d) embryo medium and (e) embryo medium. Bleaching medium contained 0.004% bleach in E3 embryo medium after diluting 10–13% active sodium chloride in embryo medium. Only viable embryos (at least 2-cell stage and no more than at the high stage, that is 3.3 h post fertilisation, with no visible deformation) were transferred into 0.2 mL PCR wells prefilled with the respective experimental medium. All experiments were approved by the Ethics committee of the University of Hull (FEC\_2019\_194 Amendment 1). Zebrafish stages are expressed in hours post fertilisation (hpf) and days post fertilisation (dpf) according to Kimmel *et al.* [50].

### Experimental design

Here, we define ‘stressors’ as environmental factors that alter homeostasis, which can be observed by measuring the behavioural, physiological and molecular adaptive responses aiming at restoring homeostasis [51–54]. We have recently shown that repeated exposure to a sublethal temperature of 32 °C is stressful to zebrafish embryos, providing the framework to study the effects of both direct heat stress and the social context of heat stress propagated *via* chemical cues [44]. We used a ‘fresh medium’ free of any metabolites and a ‘stress medium’ containing ‘social metabolites’ released by heat-stressed conspecific donors as described in Feugere *et al.* [44]. We have previously shown that media containing social metabolites from stressed embryos, control metabolites from unstressed embryos or no metabolites induce distinct phenotypes [44]. Additionally, we showed that metabolites released by unstressed zebrafish embryos are distinct—both chemically and in terms of their effects on the receivers—from those released

by heat-stressed animals [44]. For this reason, we here opted for a control free of metabolites. The factorial design yielded the following condition: control (C) or one of three ‘stress history’ treatments, namely, thermal stress (TS), social metabolites (SM) or a combined treatment (TS + SM).

One hour after collection and immediately after bleaching protocols, zebrafish embryos were individually exposed for 24 h to experimental stress history treatments, starting at 11 am during the cleavage period (2 to 3.3 hpf) until 11 am on the next day. Zebrafish embryos were exposed to a two-way factorial design of two temperature protocols (control vs. sublethal heat stress) and two types of embryo medium (200 µL of either fresh medium containing no metabolites vs. conditioned medium containing social metabolites) in a thermal cyclor with a closed lid. Temperature protocols were either (a) a control constant temperature of 27 °C or (b) thermal stress consisting of 19 cycles of temperature fluctuations between 27, 29, 32, 29 and 27 °C, with each step maintained for 15 min. Whilst deviating from realistic heatwaves, this thermal stress protocol aimed to expose embryos to a maximum number of sublethal +5 °C heat events at crucial times of embryonic development to mimic repeated stress-induced exhaustion from multiple heat events. Social metabolites were obtained by pooling 180 µL of medium per heat-stressed donor’s well into a Falcon tube and immediately transferring 200 µL of the pooled stress medium into social metabolite receivers’ wells. Fresh social metabolites for SM and TS + SM were obtained from donors exposed to TS on the day prior to limit their molecular degradation. After 24 h of exposure, embryos were removed from their treatments and exposed to a UVB/UVA damage/repair assay (Fig. 1). This assay induces deleterious mutations through UVB exposure followed by UVA-induced DNA repair. UVR treatments were labelled C + UV, TS + UV, SM + UV and TS + SM + UV. Zebrafish embryos were sampled both before (data from [44]) and immediately after UVR exposure for RNA sequencing. Another set of embryos was maintained under control conditions after UVR exposure until 4 dpf for phenotypic analyses. Embryos were humanely euthanised at 4 dpf through snap-freezing at –80 °C.

### Experimental UVR exposure

At the end of the 24-h-long exposure to C, SM, TS and TS + SM, survival rates were monitored and viable embryos were placed into small petri dishes (35 mm in diameter) in their incubation media for each treatment and were subjected to UVR in the UVB/UVA damage/repair assay. The methods were adapted from Dong *et al.* [41] and optimised for allowing > 75% survival at 4 dpf to measure differences in phenotypes between treatments (see Supplementary Methods ‘Optimisation of UVR exposure’ in Data S1). We used this sequential exposure to UVB and

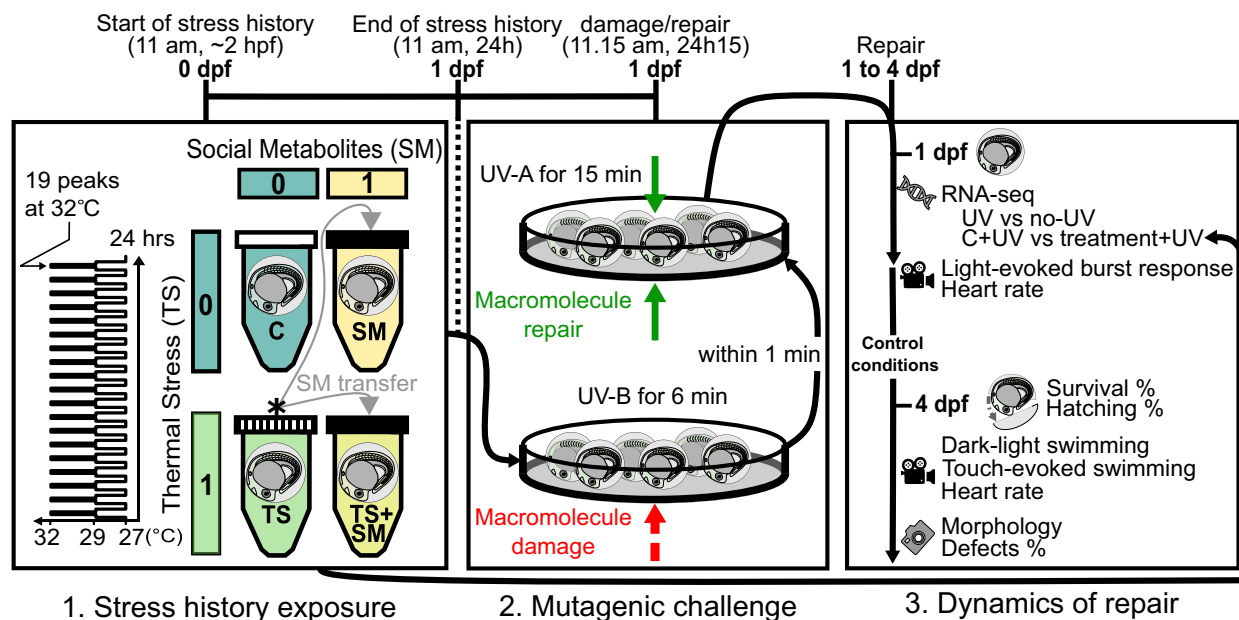


**Fig. 1.** Scheme of experimental design. Left: zebrafish embryos were exposed to heat stress history conditions of repeated thermal stress (see diagram of heat peaks) or social metabolites induced by it from 2 h post fertilisation (hpf) to 1 day post fertilisation (dpf). Stress history treatments were as follows: control (C), thermal stress (TS), social metabolites (SM), social metabolites in thermal stress (TS + SM). Grey arrows show metabolite transfer from donors (\*, hatched tube caps) to receiver embryos (black tube caps). Middle: At 1 dpf, embryos experienced successive macromolecule damage through ultraviolet B (UVB, short-dash red arrow) and repair through ultraviolet A (UVA, plain green arrows). Right: zebrafish embryos were either immediately sampled for RNA sequencing at 1 dpf (with or without UV) or incubated in control conditions for phenotypic analyses until 4 dpf. Endpoints were RNA sequencing (DNA symbol), morphology (camera), hatching (opened chorion), behaviour (video recorder) and survival.

UVA, instead of simultaneous exposure, to ensure that UVB-induced macromolecule damage that could be repaired through UVA, allowing us to study the changes in DNA repair capacity depending on stress history. The UVB/UVA damage/repair assay was first optimised on control embryos so that UVA rescued embryos from UVB-induced defects with both no excess mortality and a significant increase in healthy embryos. Zebrafish embryos within their chorion were centred in their Petri dish and exposed at 27 °C in darkness for 6 min on top of a UV transilluminator (Syngene Ltd., GelVue GVM20, Cambridge, UK) equipped with six UVB bulbs (peak of 306 nm, UVB, 8 watts lamp wattage, 1.6 watts ultraviolet output, Sankyo Denki G8T5E, Hiratsuka, Kanagawa, Japan). Next, zebrafish embryos were immediately transferred (within 1 min) to the UVA setup which consisted of a 15-min exposure at 27 °C in a 'sandwich' system of PCR handle stations (365 nm UVA, 4 W UVA output, Spectroline ENF-240C/FE) comprised of one bottom-up (direct contact against the bottom of the Petri dish) and one on top-down (11 mm away from embryos due to the height of the petri dish) UVA sources. The UVA setup was placed in the laboratory under both visible light from bulbs and natural sunlight which also excite DNA repair enzymes such as photolyases [55]. The chosen timing (6 min + 15 min)

aimed to allow the expression of DNA repair mechanisms at the time of embryo sampling for RNA sequencing (within 15 min after the end of the UVB/UVA exposure).

### RNA sequencing and analysis

RNA sequencing was performed using the same methods and sequenced at the same time as the samples described in Feugere *et al.* [44]. At the end of the stress history treatments and immediately after UVR assays, embryos still in their chorion were pooled by groups of 20 individually exposed embryos and immediately humanely euthanised by snap-freezing at  $-80$  °C. Sample sizes for RNA sequencing were  $n = 3$  biological replicate pools for each treatment, each representing the average gene expression of 20 embryos per replicate and a total of 60 embryos per treatment, obtained from different clutches. Pooling was determined as the best method to increase statistical power whilst reducing noise from individual variation in gene expression [56]. Samples were randomised, at the time of RNA extraction, for blind sample preparation and RNA sequencing. Total RNA was extracted *via* the TRIzol method followed by a DNase I digestion step (#10792877, Invitrogen™ TURBO DNA-free™ Kit, Waltham, MA, USA) and a sodium acetate clean-up. Total RNA samples

were assessed for quality, cDNA libraries were prepared with the TruSeq stranded mRNA kit, and sequenced by Illumina NovaSeq 6000, 50PE sequencing at the Edinburgh Genomics facility. FASTQC v0.11.9 (<https://www.bioinformatics.babraham.ac.uk/projects/fastqc/>) was used to assess read quality before and after filtering and trimming using FASTP v0.23.1 [57]. Reads from UV-exposed conditions were deduplicated using FASTP after PCR-biased duplication was detected using the R package DUPRADAR v1.18.0 [58]. The splice-aware mapper STAR v2.6.1 [59] served to align and count reads to the reference zebrafish genome (primary genome assembly GRCz11.104). In addition to the UV samples generated in this contribution (available under accession number GSE223685 on NCBI's Gene Expression Omnibus database), corresponding RNA sequence data from non-UV treatments (C, TS, SM, TS + SM, are available under accession number GSE220546 on NCBI's Gene Expression Omnibus database) were taken from Feugere *et al.* [44].

DESEQ2 v1.28.1 [60] was used for differential expression analyses in R v4.0.2 [61] using BIOCONDUCTOR v3.11 [62]. DESEQ2 models have been reported to successfully handle multi-factorial designs [63,64]. Therefore, transcriptomes were compared (a) for each UV- vs. no-UV treatment (C + UV vs. C, TS + UV vs. TS, SM + UV vs. SM, TS + SM + UV vs. TS + SM) and (b) between UV-treated control and treatments (C + UV vs. TS + UV, C + UV vs. SM + UV, C + UV vs. TS + SM + UV; Dataset S1). The interactive effect of combined direct heat and social metabolites was further explored by comparing SM + UV and TS + UV to TS + SM + UV (Dataset S1; see Supplementary Methods in Data S1). The magnitude of change (absolute log fold change, LFC) and gene expression ratios in response to UV were compared in a two-way design of heat × social metabolites across C + UV, SM + UV, TS + UV and TS + SM + UV. This analysis was repeated with Gene Ontology (GO)-term wide *P*-value adjustments within subsets of genes from four candidate pathways that we hypothesised to be involved in facilitating recovery from UVB: 'DNA repair' (GO:0006281), 'protein folding' (GO:0006457), 'macromolecule methylation' (GO:0043414), and 'regulation of gene expression, epigenetic' (GO:0040029). Principal Component Analyses of regularised logarithmic (*rlog*) transformed data were explored using the *prcomp* R function from the *stats* package [61]. The differentially expressed genes (DEGs) were visualised as volcano plots with the *EnhancedVolcano* R package v1.6.0 [65]. DEGs were considered significant when *P*-adj < 0.05 and |FC| ≥ 1.5 (|LFC| > 0.58). Gene identifiers were cross-database-converted using *biomaRt* R package v2.44.4 [66,67]. We retrieved the genes associated with each of the four candidate GO terms listed above using TOPGO v2.40 [68] and the org.Dr.eg.db v3.11.4 database [69]. GOSTAT v2.54.0 [70] (hypergeometric test), CLUSTERPROFILER v3.16.1 [71] and REACTOMEPA 1.32.0 [72] R packages served

to identify functionally enriched GO terms, Kyoto Encyclopedia of Genes and Genomes (KEGG) pathways and Reactome pathways associated with identified DEGs, respectively. Functional terms were considered enriched when *P*-adj < 0.1 and gene count ≥ 2.

## Phenotypic experiments

We combined different observed phenotypic variables (morphology, defects and behavioural activity) to estimate the apparent fitness of the developing zebrafish. Phenotypic measurements consisted of imaging 4-dpf larvae for morphometry and videoing for heart rate, as well as light-induced startle response (at 1 dpf) and light- and touch-evoked swimming (at 4 dpf) for behaviour. Fewer defects indicated a higher apparent fitness. Startle, light- and touch-evoked responses simulating a risk environment were used to infer on the effect of treatments on the apparent fitness of the larvae. As UV lowered developing zebrafish responsiveness to stimuli, hyperactive 1-dpf embryos (moving more) and 4-dpf larvae (swimming more) indicated a higher apparent fitness by avoiding the simulated risk (see Supplementary Methods in Data S1 for details).

## Statistical analyses

All statistical analyses were performed in R v4.0.2 [61] and graphs mainly drawn with the GGPLOT2 R package [73]. Gene expression binary data were analysed with chi-squared tests from RSTATIX v0.7.0 [74] using *chisq\_test* for model terms and *pairwise\_chisq\_gof\_test* for pairwise *post hoc* treatment comparisons. Gene expression linear models were represented with GGSCATTER from GGPUBR v0.4.0 [75]. Phenotypic data was analysed first as single univariate metrics. Binary phenotypic data were analysed using generalised linear models with binomial data. Parametric numerical data were analysed using two-way ANOVAs followed by pairwise *post hoc* tests using EMMEANS v1.7.3 [76], after transformation from BEST-NORMALIZE v1.8.2 [77,78] where necessary and possible. Model assumptions were verified using Breusch–Pagan tests for heteroskedasticity from LMTTEST v0.9-38 [79] and Shapiro–Wilks tests for normality of residuals. Nonparametric numerical data were analysed using Scheirer–Ray–Hare tests followed by pairwise Wilcoxon–Mann–Whitney *post hoc* tests from RCOMPANION v2.4.1 [80]. Since changes in morphometry (e.g. embryo size) were outcomes of treatments, we did not include them as covariates but instead tested for correlation statistics between phenotypic variables using CORPLOT v0.92 [81]. PERMANOVAs were performed with the *adonis* function from VEGAN v2.5-7 [82] followed by pairwise PERMANOVAs using the *pairwise.adonis* function from *pairwiseAdonis* v0.4 [83]. For the RNA-seq data, a PERMANOVA performed on the transformed expression matrix following a regularised log transformation (*rlog* R function from DESEQ2) helped to validate the selection of significant

DEGs by the DESEQ2 models, for which an interactive effect of the UV and stress history treatments was expected. All tests are two-tailed and multiple comparisons were adjusted for false discovery rates.

Next, the apparent fitness was investigated at the whole-body level by integrating all multivariate data from phenotypic measurements in addition to their individual analyses. Separate multivariate analyses (PERMANOVAs) were conducted on the phenotype data at 1 and 4 dpf to account for age-specific responses to UVR. Principal component analyses (PCA) of 1- and 4-dpf data were conducted using *prcomp*. Multivariate data at 1 dpf included two variables: burst activity percentage and burst count per minute. Multivariate data at 4 dpf included 14 variables: number of burst events, percentage of time moving, speed, total distance, percentage of moving larvae in the dark–light assay; total distance moved, total time moved and speed in the touch-evoked assay; as well pericardial oedema, embryo length, embryo size-normalised pericardial width, embryo size-normalised eye length, hatching and the defect score. ‘Apparent fitness scores’ were the PCA scores from the first principal components (PC1) of the multivariate data, which corresponded to 70.7% and 40.3% of the variance contribution at 1 and 4 dpf, respectively. Apparent fitness scores were recoded prior to running multivariate analyses so that higher values indicated a higher apparent fitness (i.e. moving more and having fewer mutant phenotypes, as explained above). Apparent fitness scores were compared between treatments using an ANOVA to summarise patterns within the whole of the data. Multivariate data were visualised using GGBIPLLOT v0.55 [84]. Model terms were visualised using the *plot\_model* function from sjPlot v2.8.10 [85], and trends were represented by smoothed *loess* lines using *stat\_smooth* from GGPLOT2. We reported our results with the language of evidence when the evidence is weak (i.e. a ‘trend’,  $0.1 < P < 0.05$ ) [86]. Effect sizes, given in Dataset S1, were interpreted according to Sawilowsky [87] as tiny ( $|d| < 0.1$ ), very small ( $|d| > 0.1$ ), small ( $|d| > 0.2$ ), medium ( $|d| > 0.5$ ), large ( $|d| > 0.8$ ), very large ( $|d| > 1.20$ ) and huge ( $|d| > 2.0$ ). All data can be found on Zenodo [88].

### Ethics statement

All experiments were approved by the Ethical committee of the University of Hull under the Ethics reference FEC\_2019\_194 Amendment 1.

## Results

### A common response to UVR existed in all treatments

We hypothesised that a history of heat stress amplifies the negative effects of UVR, which we tested through characterising the transcriptomic response to UVR (all

genes and functional enrichments are detailed in Dataset S1). The response to UVR was analysed by comparing each treatment followed by UVR against its non-UV counterpart (C vs. C + UV, SM vs. SM + UV, TS vs. TS + UV, and TS + SM vs. TS + SM + UV). There were 127 differentially expressed genes (DEGs) in all treatments in response to UVR, with similar directionality and expression levels (Fig. 2A and Fig. S1A). Shared genes were ascribed to macromolecule metabolic processes, nonsense-mediated decay (NMD), damage checkpoints, immune response, apoptosis/autophagy and organ development (Fig. 2C and Fig. S1B). UVR notably halved the transcription of 30 ribosomal protein subunits under all four treatments and altered the expression of heat shock proteins (*hsp70.2*, *hsp70l*, *hsp90ab1* and *hspa8*) involved in the heat shock response (HSR), at least at the RNA level.

### Different stress treatments initiated unique molecular signatures

We confirmed that in a mutagenic environment, both social metabolites and heat functioned as stressors that altered major transcriptomic pathways after UVR exposure (Fig. 3A,B,D,E and Fig. S1C–G). Compared to C + UV, heat stress in TS + UV altered 133 genes functionally enriched for eye development, somitogenesis, skeletal and cardiac muscle, macromolecule binding, but also active in the metabolism of glutathione (including the glutathione-S-transferase *gstp1*), tyrosine (involving *tyrp1a* and *tyrp1b*) and pyrimidine (Fig. 3D and Fig. S1F). Compared to C + UV, social metabolites in SM + UV induced 31 DEGs involved in fin regeneration, structural molecule activity, and keratinisation, involving several keratin-related transcripts (*krt5/17/92*, *cyt1*, *cyt11*). Social metabolites markedly upregulated two immune-related genes, *cfp* and *vsig8b* (Fig. 3B,E and Fig. S1G, Dataset S1). Comparisons within UVR treatments indicated an interactive effect of heat and social metabolites when combined, since, compared to C + UV, TS + SM + UV altered the expression of significantly more genes ( $n = 408$ ) than TS + UV ( $n = 133$ ,  $\chi^2 = 140.0$ ,  $P < 0.0001$ ) and SM + UV ( $n = 31$ ,  $\chi^2 = 324.0$ ,  $P < 0.0001$ , Fig. 3C and Fig. S1I) alone did. Whilst DEGs of TS + SM + UV were partially ( $n = 94$ ) ascribed to the response to temperature, a further 299 DEGs were uniquely found in the combined treatment TS + SM + UV and were involved in temperature response, oxidoreduction, folding activity, macromolecule binding, but also in spinal cord and blood vessel development (Fig. 3C,F and Fig. S1H,I). Comparing

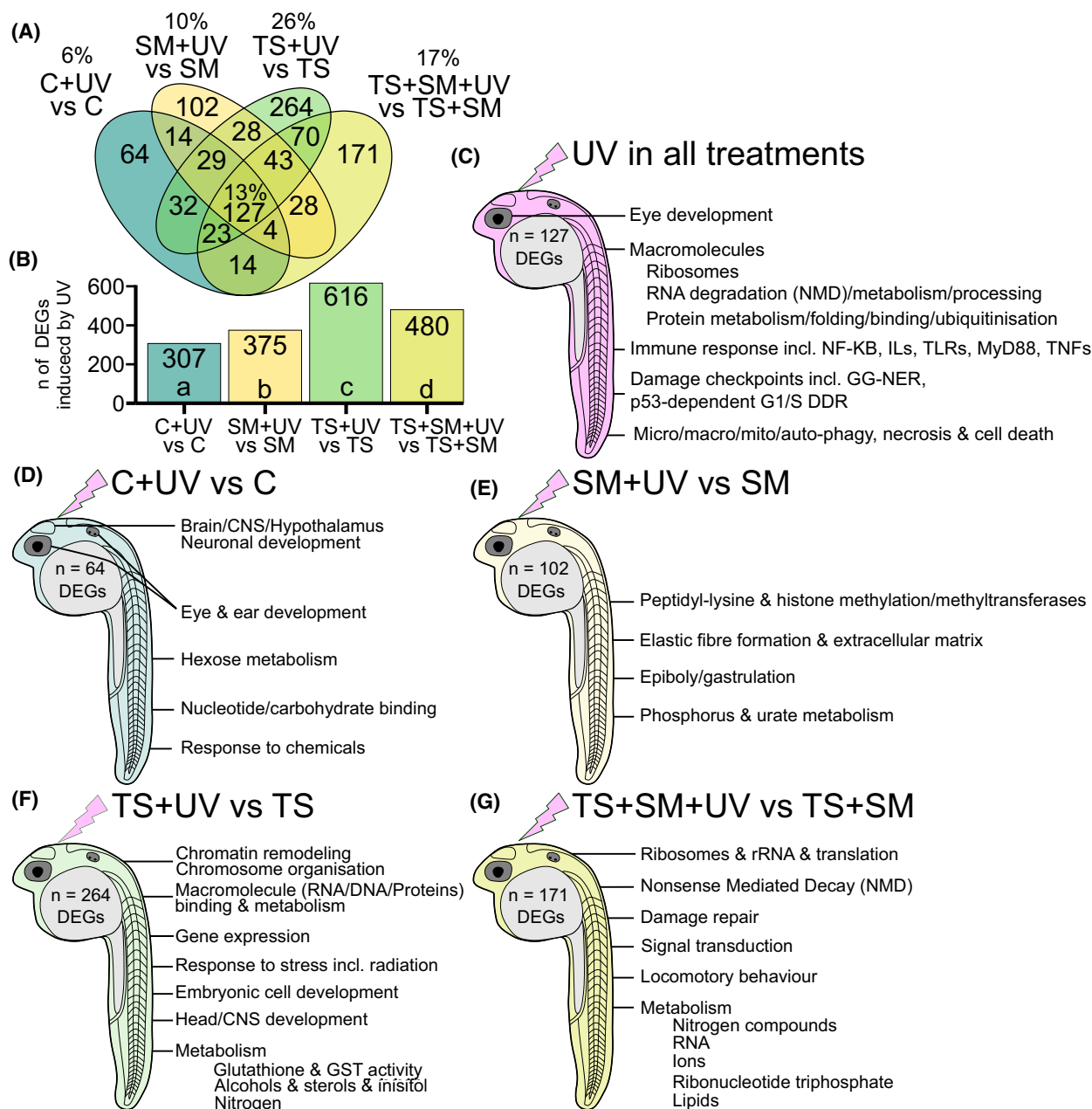


**Fig. 2.** Heat stress history potentiates the transcriptomic response to UV exposure and induces a unique transcriptomic response to UVR with different biological signatures. Transcriptomic signature of each of the four UV treatments (C, SM, TS, TS + SM) compared to their non-UV pairs. (A) Venn diagram and (B) count of significantly altered genes in response to UVR. Functional enrichment of the genes (C) shared by all four 10 treatments or (D) unique to C + UV vs. C, (E) unique to SM + UV vs. SM, (F) unique to TS + UV vs. TS and (G) unique to TS + SM + UV vs. TS + SM. Enrichments show the top enriched terms (with highest gene count/term) of Biological Processes, Molecular Functions, KEGG and Reactome pathways sorted by decreasing significance from lists of significant genes ( $P\text{-adj} < 0.05$  and  $|FC| > 1.5$ ). Treatments were C: control in fresh medium at 27 °C, SM: social metabolites at 27 °C, TS: fresh medium in thermal stress, TS + SM: social metabolites in thermal stress, all compared to their non-UV pairs. Sample size is  $n = 3$  biological replicate pools of 20 embryos per treatment.

TS + SM + UV to SM + UV and TS + UV provided further evidence for an interactive effect of heat and social metabolites in combination, altering DEGs and

pathways distinct from those activated by heat or social metabolites alone (Fig. S1J–M). The strong evidence for a large effect size of the *Treatment* term

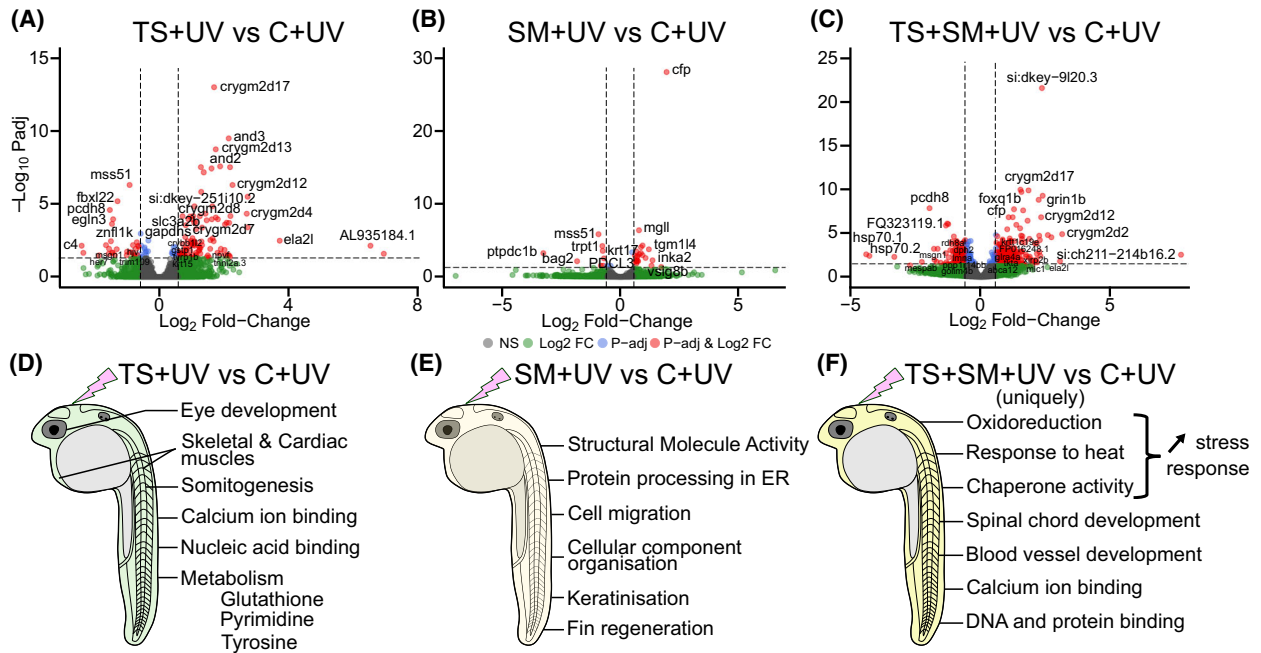


**Fig. 3.** Heat stress and social metabolites followed by UVR alter important molecular pathways. Volcano plots (upper row) showing the differentially expressed genes in response to (A) thermal stress (TS + UV vs. C + UV), (C) social metabolites (SM + UV vs. C + UV) and (E) their combination (TS + SM + UV vs. C + UV). Genes of interest are shown in red when significant ( $P\text{-adj} < 0.05$ ,  $|FC| > 1.5$ ). Genes left of the left vertical line and right of the right vertical line are underexpressed and overexpressed, respectively, compared to the control C + UV. Functional enrichments (bottom row) of transcriptomic response to TS + UV (B), SM + UV (C) and TS + SM + UV (F) compared to C + UV. Main functionally enriched terms for Gene Ontology of Biological Processes and Molecular Functions, KEGG and Reactome pathways are shown. Treatments were, after UVR exposure, C + UV: control in fresh medium at 27 °C, SM + UV: social metabolites at 27 °C, TS + UV: fresh medium in thermal stress, TS + SM + UV: social metabolites in thermal stress. Sample size is  $n = 3$  biological replicate pools of 20 embryos per treatment.

( $P = 0.001$ ; Data S1, Table S1A), validated that, compared to C + UV, stress history treatments initiated different transcriptomic signatures.

### Different stress treatments potentiated the response to UVR

Compared to C + UV vs. C ( $n = 64$  genes), stress treatments altered more genes in response to UVR. Treatment-specific UV-induced DEGs increased by 60% in SM + UV vs. SM ( $n = 102$  genes,  $\chi^2 = 8.7$ ,  $P = 0.0032$ ), quadrupled in TS + UV vs. TS ( $n = 264$ ,  $\chi^2 = 122.0$ ,  $P < 0.0001$ ) and almost trebled in TS + SM + UV vs. TS + SM ( $n = 171$ ,  $\chi^2 = 48.7$ ,  $P < 0.0001$ , Fig. 2A,B). The combined treatment TS + SM + UV vs. TS + SM induced significantly fewer treatment-specific UV-responsive genes compared to TS + UV vs. TS ( $\chi^2 = 19.9$ ,  $P < 0.0001$ ), a pattern that held true for the overall (i.e. nontreatment-specific) number of UVR-induced genes (Fig. 2A,B). The 64 genes unique to C vs. C + UV, which represent the general response to UVR, were

associated with eye, ear and brain development, hexose metabolism, response to chemicals (including peroxiredoxin *prdx1* and another heat shock protein, *hsp90aa1.2*), and nucleotide/carbohydrate binding (Fig. 2D and Fig. S1N, Dataset S1). The 102 genes unique to SM + UV vs. SM were enriched for peptidyl-lysine methylation with three notable genes, *ee1akmt2*, *smyd1b* and *suv39h1a* (Fig. 2E and Fig. S1O, Dataset S1). The 264 genes unique to TS + UV vs. TS were associated with gene expression regulation and RNA metabolism, brain and CNS development and response to stimulus, which may alter the metabolism of glutathione (including several glutathione-S-transferases *gstt1b*, *gstp1*, *gsto2* and *gstk2*), inositol phosphate, and cholesterol (Fig. 2F and Fig. S1P). The 171 genes induced by TS + SM + UV vs. TS + SM were linked to ribonucleotides, nucleotide di/triphosphates, ion homeostasis, signal transduction and also with further ribosomal deactivation (with 28 more downregulated ribosomal RNAs) and nonsense-mediated decay (NMD). Of note, TS + SM + UV also induced several locomotory and

swimming behaviour genes, namely *atoh7*, *gdpd5a*, *htr2c11*, *pleca* and *pogza* (Fig. 2G and Fig. S1Q). The strong evidence for a large effect size of the interactive term of UV and treatment ( $P = 0.001$ ; Data 1, Table S1A), validated that the response to UV depended on the level of stress history treatment at the transcriptomic level.

### Candidate UV-induced pathways

Stress history-dependent responses to UVR were further explored within candidate pathways associated with macromolecule processing: ‘RNA integrity Number’ (RIN), ‘DNA repair’ (GO:0006281), ‘protein folding’ (chaperone response, GO:0006457), ‘regulation of gene expression, epigenetic’ (GO:0040029) and ‘macromolecule methylation’ (GO:0043414). All statistical analyses are reported in Dataset S1. Overall, there was no evidence that heat ( $F = 0.01$ ,  $P = 0.9192$ ) and social metabolites ( $F = 0.18$ ,  $P = 0.6750$ ) had an effect on RNA degradation (Fig. S2A), whilst UVR ( $F = 6.44$ ,  $P = 0.0195$ ) degraded RNA, as evidenced by lowered RIN values. Two DNA repair genes, *eyal* and *fancf*, were respectively down- and upregulated in all treatments in response to UVR (Fig. 4A,B). Heat stress, but not social metabolites, increased the number ( $n = 19$  vs. 7 genes,  $\chi^2 = 5.54$ ,  $P = 0.0186$ ) and expression magnitude ( $H = 4.23$ ,  $P = 0.0397$ , ‘very small effect size’  $|d| = 0.11$ ) of DNA repair genes, in response to UVR (Fig. 4C).

We expected that heat stress history would limit DNA repair capacities. However, TS + UV vs. TS upregulated six (*adprh12*, *cry5*, *nthl1*, *prmt6*, *rmi2* and *ube2al*), and downregulated one (*zfyve26*), DNA repair genes not found in C + UV vs. C. One DNA repair gene, *apex2*, was significantly upregulated under all stress treatments but not in C + UV vs. C (Fig. 4B). Two DNA repair genes were associated only with social metabolites, with *brp1* downregulated by UV in SM + UV vs. SM and *rps3* downregulated in both social metabolite treatments (TS + SM + UV vs. TS + SM and SM + UV vs. SM but not in TS + UV vs. TS; Fig. 4B). Furthermore, deviation from the 1-to-1 expression ratio in ‘treatments with UVR’ vs. ‘treatments without UVR’, compared to C + UV vs. C, evidenced perturbations of the DNA repair pathway by treatments (Fig. 4D–F). UV-induced chaperone responses were overall consistent in all treatments both in terms of number of genes and expression magnitude, which were not altered by heat ( $\chi^2 = 1.47$ ,  $P = 0.2250$  and  $F = 0.2$ ,  $P = 0.6736$ ) nor medium ( $\chi^2 = 0.02$ ,  $P = 0.8930$  and  $F = 0.0$ ,

$P = 0.9862$ , Fig. S2B–G). Seven shared chaperone-related genes included three HSPs (*hsp70l*, *hsp90ab1* and *hspa8*), but also *dnajb1b*, *ppiaa*, *tbcc* and *zgc:122979* (an HSP 40 family member and human orthologue of DNAJB5, Fig. S2B–F). The expression of several hallmark genes, such as *hsp70.3*, *hsp90aa1.2*, *fkbp1b*, *dnajb1* and *dnaja1b*, in TS + SM + UV vs. TS + SM was not as strong as the control response to UV in C + UV vs. C; or was already activated by heat stress (without UVR) but not further increased by UVR (Fig. S2F,G). Particularly, *hsp70l* increased by 200-fold in C + UV vs. C, but only sixfold in TS + SM + UV vs. TS + SM, representing a 33-fold drop in its expected UVR induction (Fig. S2G). Overall, the proportion and the magnitude of expression of genes involved in the macromolecule methylation pathway were similar in response to UVR in all four treatments (Fig. S2H–M). Nonetheless, social metabolites had an effect on protein methylation as SM + UV vs. SM altered transcript levels of three protein methyltransferases (*suv39h1a*, *eef1akmt2* and *smyd1b*) not found in C + UV vs. C (Fig. S2H,I). Investigating epigenetic-associated genes (Fig. S2N–R) revealed that social metabolites ( $\chi^2 = 5.0$ ,  $P = 0.0253$ ), but not heat stress ( $\chi^2 = 0.2$ ,  $P = 0.6550$ ), activated several epigenetic regulators, with four genes found in social metabolites treatments: *bmi1b*, *srvt*, and two histone linkers, *h1-0* and *si:ch73-368j24.12* (human orthologue: H1.5 linker histone; Fig. S2N). Social metabolites also altered the expected 1-to-1 expression ratios of epigenetic pathway genes between SM + UV vs. SM and C + UV vs. C ( $R = 0.18$ ,  $P = 0.098$ , Fig. S2P). Of note, heat marginally tended (weak evidence:  $P < 0.1$ ) to increase the magnitude of gene expression of both methylation and epigenetic processes (Fig. S2J,O).

### Heat rescued phenotypes from UVR, whilst social metabolites caused hypoactivity and TS + SM overwhelmed larvae

There were no differences in mortality, with > 95% of embryos surviving the UVR exposure regardless of treatments (Fig. S3A). We tested the hypothesis that heat stress history causes more mutant phenotypes in response to UVR through measuring fitness-relevant outcomes (Fig. 5A–E). All statistical analyses are reported in ‘Statistics’ in Dataset S1. The 1-dpf multivariate data showed that both heat ( $F = 28.04$ ,  $P = 0.001$ ) and social metabolites ( $F = 9.14$ ,  $P = 0.001$ ) altered 1-dpf startle behaviours, with significant differences between TS + UV ( $F = 7.78$ ,  $P = 0.006$ ) and TS + SM + UV ( $F = 34.74$ ,  $P = 0.006$ ) compared

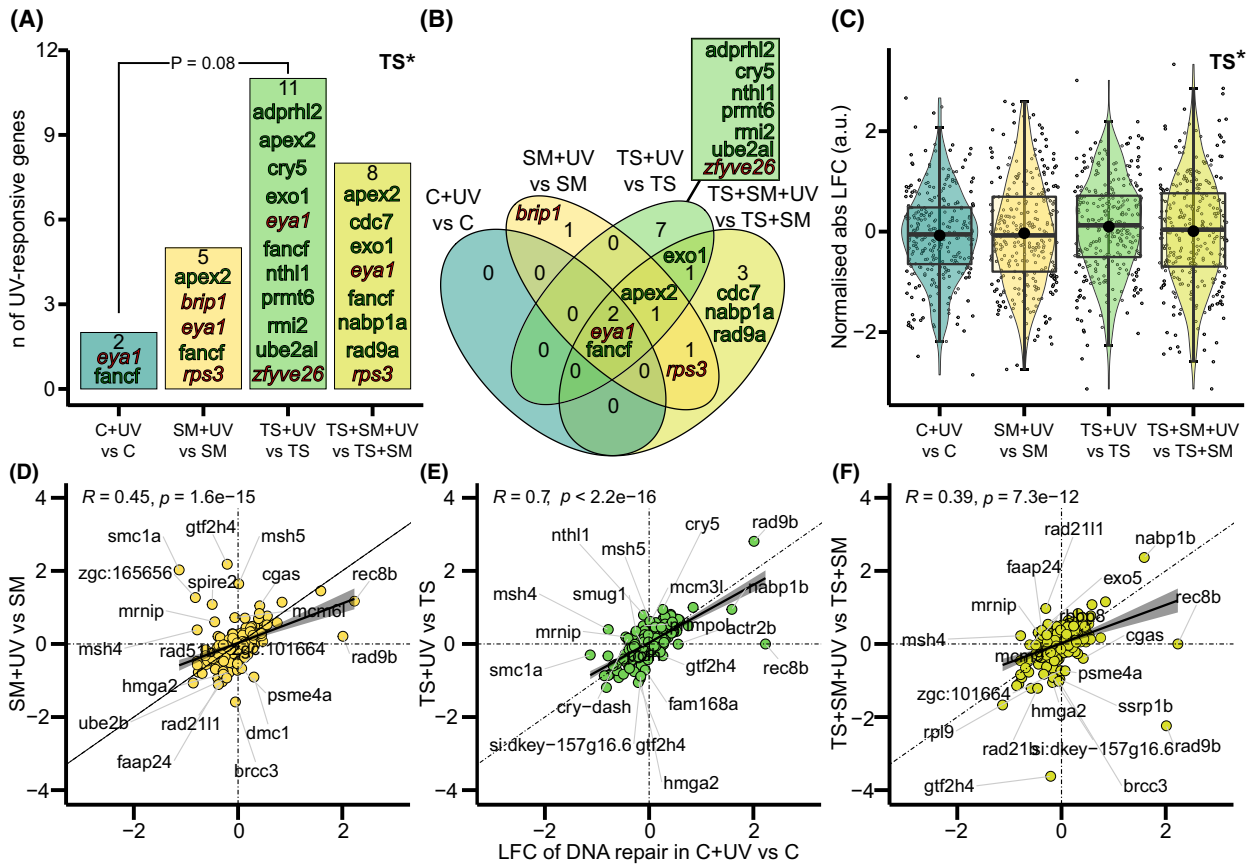


**Fig. 4.** Influence of stress history treatments on DNA repair genes in response to UVR. (A) Counts and (B) Venn diagram of significant genes from DNA repair (GO:0006281,  $n = 288$  genes) in each treatment in response to UVR. Nonitalicised dark green and italicised dark red gene names, respectively, indicate up- and downregulation (GO term wide  $P$ -adj  $< 0.05$  and  $|FC| > 1.5$ ). (C) Magnitude of UV-induced DNA repair gene expression changes represented by the normalised absolute log-fold change (LFC). Heat stress (TS) is a significant predictor shown on top-right corners in A (chi-squared test) and C (Scheirer–Ray–Hare test) with \* indicating  $P < 0.05$ . Bottom row: LFC of gene expression in DNA repair pathway in (D) SM, (E) TS and (F) TS + SM stress history treatments (y-axes) versus control C (x-axes). The null hypothesis is that the UV-induced repair response is similar for all treatments and respects a 1-to-1 ratio (diagonal lines). Solid black lines and shaded areas depict linear fits and confidence intervals. Labels indicate the top 20 genes with the most pronounced deviation relative to C. Treatments were, before and after (+UV) UVR exposure, C: control in fresh medium at 27 °C, SM: social metabolites at 27 °C, TS: fresh medium in thermal stress, TS + SM: social metabolites in thermal stress all compared to their non-UV pairs. Sample size is  $n = 3$  biological replicate pools of 20 embryos per treatment.

to C + UV (Fig. 5A). 1-dpf embryos in TS + SM + UV behaved differently from SM + UV ( $F = 17.99$ ,  $P = 0.006$ ) and TS + UV ( $F = 8.27$ ,  $P = 0.024$ ). Conversely, the 4-dpf multivariate data showed that only TS + UV differed from C + UV ( $F = 5.62$ ,  $P = 0.03$ ), with only weak evidence that TS + UV also deviated from SM + UV ( $F = 4.72$ ,  $P = 0.078$ ) and TS + SM + UV ( $F = 4.69$ ,  $P = 0.066$ , Fig. 5B).

We then individually analysed phenotypic variables at 1 and 4 dpf (Fig. S3). Both heat stress ( $H = 38.1$ ,  $P < 0.0001$ ) and social metabolites ( $H = 3.96$ ,  $P = 0.0465$ ) reduced light responsiveness in 1-dpf embryos (Fig. S3E,F), with TS + UV ( $W = 457$ ,

$P = 0.0009$ ) and TS + SM + UV ( $W = 661$ ,  $P < 0.0001$ ) lowering burst activity % compared to C + UV (Fig. S3E). Larvae in SM + UV ( $t = -2.3$ ,  $P = 0.0491$ ) and TS + UV ( $t = 3.8$ ,  $P = 0.0016$ ) were longer relative to C + UV (Fig. S3G). In turn, heat stress ( $z = 2.8$ ,  $P = 0.0051$ ) facilitated hatching, with an increase from 11% in C + UV to 50% in TS + UV ( $z = -2.8$ ,  $P = 0.0306$ , Fig. S3B). There was weak to moderate evidence that social metabolites ( $F = 4.9$ ,  $P = 0.0287$ ) and heat (a trend with  $F = 2.9$ ,  $P = 0.0945$ ) altered the 4-dpf embryo size-normalised pericardial width (Fig. S3J). Larvae in TS + UV had narrower pericardia relative to their body sizes compared to C + UV ( $t = 2.91$ ,  $P = 0.0104$ ) and SM + UV

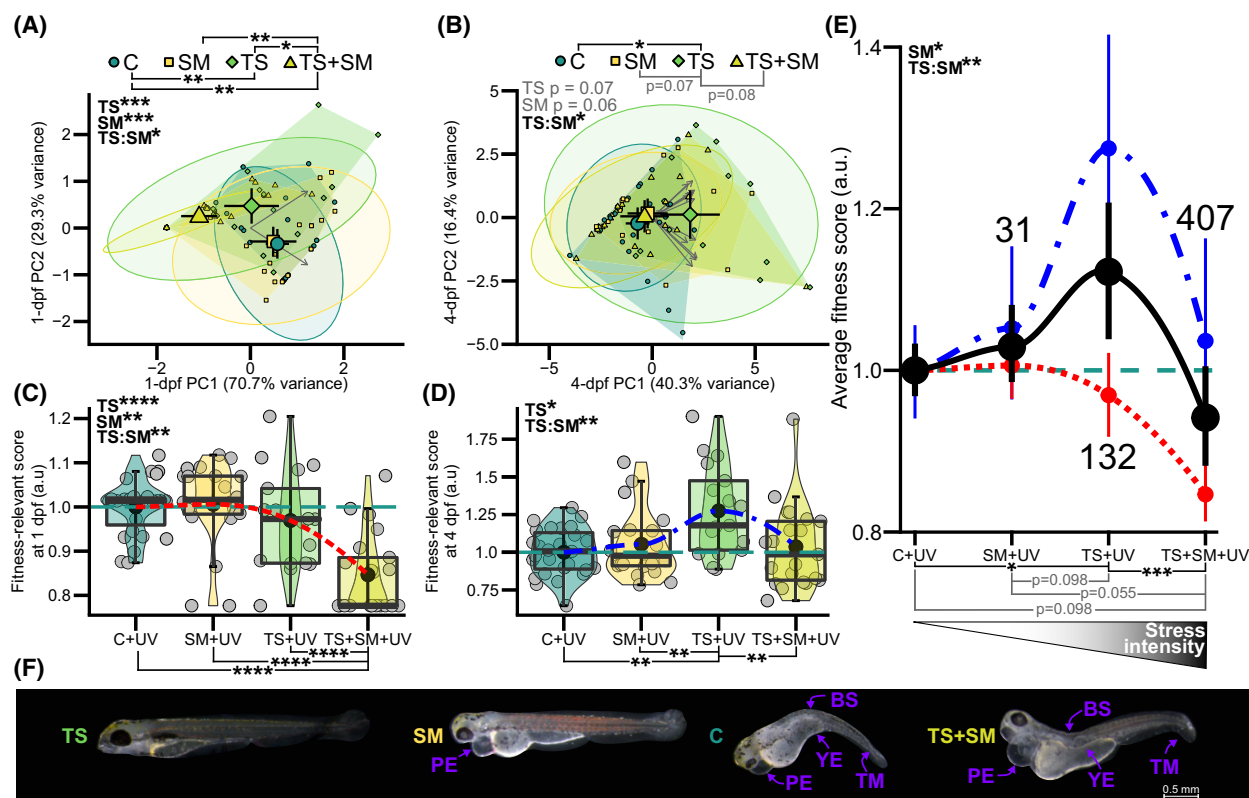


**Fig. 5.** TS + UV outperformed C + UV and TS + SM + UV showing a nonlinear response to ultraviolet radiation (UVR) with stress intensity. Principal component analyses of phenotypes at 1 (A) and 4 (B) days post fertilisation (dpf). Higher values along PC1 indicate higher apparent fitness scores. Large and small coloured symbols show centroids ( $\pm 95\%$  confidence interval, CI) and individual scores, respectively. Ellipsoids show 95% normal CI probabilities. Polygons show smallest areas clustering samples per treatment. Apparent fitness scores are shown at 1 (C) and 4 (D) dpf. Boxes show median and 25–75% quartiles. Whiskers are min/max values within 1.5 interquartile range. Individual data given as jittered grey circles. (E) Apparent fitness scores (means  $\pm$  SEM) averaged between 1 and 4 dpf. Smooth *loess* lines show 1-dpf (dotted red line), 4-dpf (dot-dashed blue line) and average (black solid line) scores. Black dots show mean  $\pm$  SEM in arbitrary units (a.u.) scaled to control (C + UV, dashed blue horizontal lines). Numbers in (E) show how many genes were altered compared to C + UV. Significant two-way model terms are shown in top-left corners with TS = thermal stress and SM = social metabolites. *Post hoc* comparisons are shown with horizontal bars. (F) Compared to C + UV, embryos have fewer defects and are longer in TS + UV but show larger pericardial-to-embryo length ratios with social metabolites SM + UV and TS + SM + UV. Defects include bent spine (BS), pericardial oedema (PE), tail malformation (TM) and yolk extension disruption (YE). Image modification: embryo images were selected to represent treatment effects and manually detoured, contrast was adjusted evenly for all treatments, and put on a black background. All tests are two-tailed with adjustment for false discovery rate when multiple comparisons are made. Treatments were all followed by UVR (+UV), with C + UV: control in fresh medium at 27 °C ( $n = 28$ ), SM + UV: social metabolites at 27 °C ( $n = 22$ ), TS + UV: fresh medium in thermal stress ( $n = 20$ ), TS + SM + UV: social metabolites in thermal stress ( $n = 25$ ). \*:  $P \leq 0.05$ , \*\*:  $P \leq 0.01$ , \*\*\*:  $P \leq 0.001$ , \*\*\*\*:  $P \leq 0.0001$ . Weak evidence ( $P < 0.1$ ) is shown in grey. See Fig. S3 for the analysis of individual metrics.

( $t = 2.87$ ,  $P = 0.0104$ ). There was strong evidence for protective effects against pericardial oedema with heat stress ( $z = -3.3$ ,  $P = 0.0010$ ), with a drastic decline in pericardial oedemas only in TS + UV (32%,  $z = 3.3$ ,  $P = 0.0059$ ) compared to C + UV (82%, Fig. S3C)—although heart rates remained similar across treatments (Dataset S1). Larvae exposed to TS + UV also had the lowest overall defect score, albeit not significant relative to C + UV (Fig. S3I). Heat stress ( $F = 8.27$ ,  $P = 0.0051$ ) also significantly increased the eye-to-body size ratio following exposure to UVR

(Fig. S3H). At 4 dpf, there was weak to moderate evidence that social metabolites reduced the dark–light swimming activity ( $H = 3.86$ ,  $P = 0.04955$ , Fig. S3K), swimming burst counts ( $H = 3.37$ ,  $P = 0.0663$ , Fig. S3M) and touch-evoked swimming speeds ( $F = 3.64$ ,  $P = 0.0599$ , Fig. S3P). Conversely, despite having experienced UV, 4-dpf larvae in TS + UV were constantly most responsive and had the highest number of active larvae (Fig. S3D), activity % (Fig. S3K), distance swum (Fig. S3L), burst count (Fig. S3M) and speed (Fig. S3N) in response to light, but also the

highest distance swum (Fig. S3O) and speed (Fig. S3P) in response to touch.

The morphological consequences of exposure to TS + UV were associated with higher swimming responsiveness with positive (embryo size) and negative (pericardial oedema, pericardial width and defect scores) relationships. Conversely, embryos in the combined treatment TS + SM + UV did not show the developmental rescue effect conferred by heat, and were smaller compared to TS + UV ( $t = 3.3$ ,  $P = 0.0035$ ) and SM + UV ( $t = 1.89$ , trend with weak evidence:  $P = 0.0937$ ), reaching similar sizes as in the control C + UV ( $t = -0.32$ ,  $P = 0.7474$ , Fig. S3G). The heat-induced protection against wide pericardia was lost in TS + SM + UV compared to TS + UV ( $t = -3.11$ ,  $P = 0.0104$ ), resulting in similar pericardial width relative to C + UV ( $t = -0.35$ ,  $P = 0.8889$ , Fig. S3J). This caused twice as much pericardial oedema (although with weak evidence,  $z = -2.12$ ,  $P = 0.1008$ , Fig. S3C) in conjunction with higher defect scores ( $W = 116$ ,  $P = 0.0490$ , Fig. S3I) in TS + SM + UV compared to TS + UV. Likewise, TS + SM + UV caused the lowest responsiveness to light at 1 dpf (Fig. S3E,F) and to light and touch stimuli at 4 dpf (Fig. S3K–P). Altogether, this indicated that the combined treatment TS + SM + UV induced more defects and negative outcomes compared to TS + UV.

Summarising the multivariate data into an ‘apparent fitness score’ (where higher values indicate better apparent fitness-relevant outcomes) confirmed that TS + SM + UV performed worst compared to C + UV ( $t = 5.92$ ,  $P < 0.0001$ ), SM + UV ( $t = 5.72$ ,  $P < 0.0001$ ) and TS + UV ( $t = 4.22$ ,  $P < 0.0001$ ) and displayed the lowest apparent fitness scores at 1 dpf (Fig. 5C). On the other hand, TS + UV increased apparent fitness scores at 4 dpf compared to C + UV ( $t = -3.47$ ,  $P = 0.0049$ ), SM + UV ( $t = -2.54$ ,  $P = 0.0257$ ) and TS + SM + UV ( $t = 3.05$ ,  $P = 0.0094$ , Fig. 5D). Overall, the average apparent fitness scores peaked with TS + UV, which had the highest average apparent fitness score, higher than C + UV ( $t = -2.51$ ,  $P = 0.0422$ ) and TS + SM + UV ( $t = 3.9$ ,  $P = 0.0010$ ). The average apparent fitness score dropped in the multistress treatment TS + SM + UV, which tended to have lower scores compared to C + UV ( $t = 1.76$ , weak evidence:  $P = 0.0983$ ) and SM + UV ( $t = 2.24$ , weak evidence:  $P = 0.0550$ , Fig. 5E). In summary, this revealed: (a) that compared to C + UV control, larvae in SM + UV grew longer but were hypoactive at 4 dpf, (b) that larvae in TS + UV showed less pericardial oedema and developed faster, which facilitated their hatching and improved their behavioural

responses at 4 dpf, (c) whilst embryos and larvae in TS + SM + UV failed to limit the formation of pericardial oedema and had the worst apparent fitness performances. This indicated a nonlinear relationship between apparent fitness in response to UVR and the intensity of stress history (Fig. 5E).

## Discussion

Early-life stress may incur carry-over effects [89] lowering the capacity of an organism to cope with future stress events [90–92]. This raises concerns for the fate of species inhabiting increasingly challenging aquatic environments, particularly given social contexts amplify stress levels [44]. Therefore, we explored the effects of early-life stress history on the UVA-catalysed recovery from UVB-induced damage in zebrafish embryos. UVR can cause oxidative stress toxic to lipids, antioxidants, ribosomes, proteins and nucleic acids [5,38,93]. Here, UVR altered the metabolism of macromolecules (ribosomes, mRNA, protein), DNA checkpoints and organ development. The unfolded protein response and ubiquitination pathways protect proteins and remove damaged ones [94,95], likely explaining their activation by UVR in our study. UVR lowered RNA integrity and activated nonsense-mediated mRNA decay and DNA checkpoints, indicating that UVR caused damage to nucleic acids. The DNA repair response involved *fancf* and *eyal* in all treatments. *fancf* helps recruit DNA repair genes upon DNA damage [96–98]. Moreover, *eyal* is a DNA repair-promoting, UVR-inducible enzyme that was downregulated by UVR, which is indicative of genotoxicity [99–101]. Many cell components were altered by UVR, likely causing autophagy to remove damaged macromolecules [102]. These cellular effects escalated to the organismal level, resulting in hypoactivity, teratogenicity and reduced hatching, as previously reported in zebrafish embryos [38,103].

Direct heat stress changed this UVR damage/repair response compared to UVR-exposed control embryos. Heat-stressed larvae were longer with fewer pericardial oedema, better swimming performances, and earlier hatching, providing evidence that heat rescued and/or protected embryos from UVR damage. These results do not support our initial hypothesis that heat stress would disadvantage embryos in a mutagenic environment. Our results align with concepts of ‘hormesis’ or ‘cross-protection’, that refer to beneficial stimulating effects of low-dose, often mild, initial stress [11,104,105]. In our study, the heat hormetic effect rescuing embryos from UVR may have resulted from heat-induced defence mechanisms protecting against

and/or repairing irradiation damage. Comparing transcriptomes of heat-stressed embryos before and after the UVR damage/repair assay suggests that hormesis may have been mediated *via* (a) a stage-dependent increased baseline tolerance, and by stimulating (b) antioxidants, (c) the heat shock response and (d) DNA repair.

Heat-stressed embryos were 6 h older than control embryos that were still undergoing segmentation when UVR started [44]. Older heat-stressed embryos may display different phenotypes from stage-matched controls [7], which warrants future research to disentangle the effects of heat and development in the observed response to UVR. Mature fish are more resistant to UVR than earlier stages, possibly through a protective role of pigmentation [5,14,103]. Heat treatment upregulated two genes (*tyrp1a/b*) involved in melanin synthesis [106,107], which may shield cells from UVR [108]. Overdeveloped heat-treated embryos may also have benefited from energy supply from the yolk sac [109]. Likewise, heat upregulated several genes involved in glycolysis (e.g. *gapdh*, *gpi*, *pkmb*) and energy metabolism [44]. Therefore, heat-stressed embryos may mobilise energy to fuel ATP-dependent DNA repair mechanisms such as nucleotide excision repair [110] and mismatch repair [35,111]. Supporting this, heat-stressed embryos were hypoactive immediately after UVR, suggesting that they may have redirected energy towards UVR-coping strategies.

Antioxidants may mediate hormesis through preparation for oxidative stress, an adaptive physiological mechanism that upregulates antioxidants to confer tolerance against stress-induced reactive oxygen species [112–114]. Supporting this, heat stress upregulated several glutathione-S-transferases (GSTs) following UVR. GSTs play a key role in the defence against oxidative stress by catalysing the binding of reduced glutathione to damaged macromolecules (lipids, DNA and proteins), marking them for degradation [34,115]. The heat shock response may mediate hormesis by limiting molecular damage [116,117]. Our heat stress protocol activated the heat shock response at 1 dpf [7,44], which may have provided heat-treated embryos with a reserve of HSP transcripts ready to be translated once UVR started. HSPs are also key modulators of DNA repair genes, which may in turn favour cell survival [118]. Furthermore, heat activated the ubiquitin-proteasome system (UPS, involving several ubiquitins, e.g., *ube2a*, *otulina*, *igs15* and *otud7b* genes), which play a central role in DNA repair [119]. Therefore, the cellular stress response activated by both heat and UVR may have acted as a short-lived ‘transient cross-protection’ resulting in the cross-tolerance against UVR [11].

Unexpectedly, we found that heat stress history improved DNA repair capacity in response to UVR. These findings agree with increased DNA repair rates at high temperature in *Daphnia pulicaria* [120], tadpoles *Limnodynastes peronii* [121] and zebrafish embryos [122]. DNA damage not repaired within 2 h is irreversible in zebrafish embryos [32], suggesting that transcriptomic changes captured approximately 30 min following UVR played a key role in mediating hormesis. Whilst control embryos had limited DNA repair capacity activating only one DNA repair gene (*fancf*), heat upregulated several DNA repair genes. Likewise not supporting the initial hypothesis, we found a more competent heat-induced photorepair indicated by the upregulation of *cry5*, a 6–4 photolyase, that may have acted against UVR damage at the time of (UVA and blue) light exposure in TS + UV, possibly explaining the higher survival in response to UVR [33,55,123–125]. Heat also upregulated other DNA repair-related genes that may have helped embryos in TS + UV to repair DNA damage: *adprhl2*, *apex2*, *exo1*, *nthl1*, *rmi2* and *ube2a* (Table 1).

Likewise, heat stress activated the metabolism of inositol phosphate, which is known to stimulate double-strand break repair through nonhomologous end joining [141]. Furthermore, heat stress tended to increase the expression of transcripts involved in epigenetics and methylation. Histone methylation can transmit heat hormetic effects to later life stages and subsequent generations [142], which may mean that heat-treated embryos not only perform better in response to UVR, but could also be better protected from subsequent stress events.

Overall, heat stress history rescued and/or protected embryos from molecular damage in a mutagenic environment, likely by chaperoning proteins, activating DNA repair, stabilising the genome and facilitating methylation and epigenetic regulation. Whilst our findings align with the concept of hormesis wherein heat protects cells by activating the proteasome, the heat shock response and antioxidants [116,143], further research is needed to discriminate the involvement of protective versus repair pathways in the hormetic effect observed here. We also acknowledge limitations to using behaviour and morphology as fitness proxies [144–146], warranting future studies to assess whether these fitness advantages hold in the natural environment, particularly if hormesis is mostly mediated by the transient cellular stress response, as discussed in Rodgers and Gomez Isaza [11]. The possible loss of thermal plasticity and UVB tolerance in laboratory-adapted zebrafish strains [41,147] and the low percentage of explained variance (40.3%) in the 4-

**Table 1.** Genes involved in DNA repair mechanisms (GO:0006281) that were upregulated in zebrafish embryos exposed to direct heat stress prior to UV.

Gene	Role	References
<i>adprh2</i>	Prevents cell death by removing poly-ADP ribose accumulated following oxidative stress	[126]
<i>apex2</i>	Limits DNA damage by preventing the stabilisation of UV-induced DNA cleavage	[127–129]
<i>exo1</i>	Mediates a faster DNA mismatch repair pathway	[130]
<i>ntlh1</i>	Cleaves oxidative pyrimidine damage during base excision repair	[131]
<i>prmt6</i>	Methyltransferase preventing apoptosis and rescuing embryogenic defects, and regulating DNA polymerase and DNA repair genes	[132–134]
<i>rmi2</i>	Promotes genome stability within the Bloom syndrome (BLM) complex, involved in homologous repair	[135–137]
<i>ube2a</i>	E2 ubiquitin-conjugating enzymes such as <i>ube2a</i> mediate protein ubiquitination promoting DNA repair and genome integrity	[138–140]

dpf phenotypic data also warrant repeated experiments validating our findings using wild zebrafish lines. Of note, severe heat exacerbates stress-induced damage, following an inverted U-shaped dose–response curve [105,143,148]. The positive outcome of heat stress observed here is likely explained by the sublethal heat regime we used. We hypothesise that temperatures beyond 32 °C would instead lead to negative outcomes in a mutagenic environment, which again warrants further investigation.

Biotically stressed aquatic animals communicate with naive neighbours [149–151]. We previously extended this mechanism to abiotic stress and identified specific classes of social metabolites induced by heat stress [6,7,44]. Here, we again confirm that social metabolites of heat-stressed donors induce stress in receivers, through activating immune-, cell structure- and keratin-related genes. Similar to the effect of direct heat stress, embryos in SM + UV were hypoactive at 1 dpf and longer at 4 dpf, but the activated molecular pathways were markedly different from those activated by heat stress. Stress treatments, including social metabolites, but not control conditions, activated *apex2*, an important DNA repair gene in embryogenesis [127,152]. Keratin genes activated by social metabolites may have improved photoprotection against DNA damage in keratinocytes [153,154] and promoted repair of DNA breaks [155]. However, the response to UVR in the social metabolite treatment

also downregulated both *brip1* and *rps3*, suggesting some level of DNA damage [156,157] that may have caused the observed malformations. Social metabolites altered epigenetic and methylation genes, which may mediate downstream transcriptomic changes [158]. For instance, SM + UV downregulated *srvt*, which plays a role in DNA repair [159,160], histone h1-5 and methyltransferases, suggesting alterations in transcriptional regulation [161,162]. One differentially expressed gene was *smyd1b*, playing a key role in skeletal muscles [163,164], the downregulation of which may explain how social metabolites rendered embryos hypoactive. Therefore, whilst social metabolites induced markedly more responsiveness to UVR compared to controls, just like heat stress did, they failed to protect embryos against UVR damage as efficiently as heat stress. Whilst the effects observed in the social metabolite treatment could be ascribed to specific metabolites induced by heat, similar to what we reported previously [7,44] we cannot exclude that this bouquet of cues [44] also includes regularly excreted, nonheat-specific social cues. Ideally, cues from unstressed conspecifics should be included in all future experiments as a better-suited control [151] to confirm the involvement and consequences of heat-induced vs. regular social metabolites in mutagenic environments.

The finding that heat stress alleviated the response to UV is in line with a net antagonistic response of multiple stressors in freshwater environments [165]. However, a striking finding from our study is that this was no longer true when adding another layer of complexity: the social context of stress. In effect, the treatment combining heat stress within a social context profoundly altered the transcriptome both before [44] and after UVR exposure. One possible explanation for this is that single exposure to either direct heat, or social metabolites, influenced distinct pathways in response to UVR, which would both be activated in the combined treatment. These embryos experienced increased stress levels as suggested by more stress-related functional changes, further damage to RNA, and more inhibition of translation by downregulating ribosomal RNAs. The combined treatment elevated HSP levels before UVR [44]. Such elevated basal HSP mRNAs may have attenuated the heat shock response to subsequent acute stressors [90,166]. Supporting this idea, the combined treatment limited and/or inhibited the upregulation of key HSPs in response to UVR, likely lowering protection against protein damage. The interacting effect of heat and social metabolites amplifying transcriptome changes also likely cost more energy, as suggested by more pronounced behavioural hypoactivity. Overall, our data suggest that the

combination of direct heat with social metabolites was a stronger stressor that prevented embryos from activating the heat hormetic effect and shifted the dose–response towards negative outcome. It may follow that in a natural environment, where embryos in a clutch exchange social metabolites, any protective hormetic effect of heat will be negated by the presence of social metabolites exchanged between clutch mates. Of note, we raised zebrafish embryos in darkness, which may have delayed their normal embryonic development [167], warranting future studies with ecologically realistic conditions to better comprehend the social context of stress in fish embryos.

## Conclusion

Our findings that heat stress may have protective effects in mutagenic environments, and the mechanisms we observed at the molecular level, are significant for the community of researchers focusing on the combined effects of stressors in natural environments, as cross-protection may facilitate ‘pre-adaptation’ for organisms facing increasing anthropogenic stressors [11]. However, the fact that social contexts superimposed to heat stress limit the capacity of aquatic organisms to cope with stressful environments is highly relevant for natural populations experiencing increasingly common heat and mutagenic stressors exacerbated by climate change [168,169]. The consequences of such altered fitness under UV may carry over to later life stages [19,28] and scale up to ecosystem levels [13]. Most importantly, we report that the social aspect of stress adds a layer of complexity to rising concerns on the effects of UV across diverse aquatic and terrestrial habitats harbouring vulnerable groups such as fish and amphibians [13,15]. Our results suggest that species that are found or raised in high densities would be disadvantaged in stressful environments if they face both stressors within social contexts during early-life stages. Whilst confined to laboratory settings, we provide a solid basis to understand the consequences of stress and social history in mutagenic environments and we emphasise on the need to consider species’ social contexts to better predict their response to global changes.

## Acknowledgements

We thank the technical staff from the Biology and Marine Sciences department at the University of Hull for providing us with the equipment for experimental ultraviolet exposure. We would like to thank Emma Chapman and Robert Donnelly from the University of

Hull for support in the transcriptomic analyses. We would like to thank Alan Smith for fish care in the aquarium facility at the University of Hull. We acknowledge the Viper High Performance Computing facility of the University of Hull and its support team. We thank in particular Chris Collins and Darren L. Bird for their help. We thank the anonymous Reviewers for their valuable feedback. Funding was provided by the University of Hull within the MolStressH<sub>2</sub>O cluster to LF, PB-A and KCWV and the Royal Society (RGS\R2\180033) to KCWV. Funded by the European Union (ERC/CoG, MolStressH<sub>2</sub>O—101044202). Views and opinions expressed are however those of the author(s) only and do not necessarily reflect those of the European Union or the European Research Council Executive Agency. Neither the European Union nor the granting authority can be held responsible for them.

## Author contributions

KCWV and PB-A conceived and designed the project. LF acquired experimental data. LF, AB, CSDF and KCWV analysed the data. LF, KCWV, PB-A and KBS interpreted the data. KCWV and PB-A supervised the study. LF wrote the first draft of the manuscript, and KCWV, AB, CSDF, PB-A and KBS critically reviewed the manuscript and contributed its final version.

## Peer review

The peer review history for this article is available at <https://www.webofscience.com/api/gateway/wos/peer-review/10.1002/1873-3468.70047>.

## Data accessibility

The data from phenotypic experiments, processed transcriptomic data and custom code (R scripts and bioinformatic pipelines) are available on Zenodo (10.5281/zenodo.7566285) and on NCBI Gene Expression Omnibus under the accession number GSE223685. The raw transcriptomic data of the embryos not exposed to UVR is retrieved from Feugere *et al.* [44] and is available on NCBI Gene Expression Omnibus under the BioProject PRJNA910181 and the accession number GSE220546.

## References

- 1 IPCC (2019) IPCC Special Report on the Ocean and Cryosphere in a Changing Climate. Intergovernmental Panel on Climate Change.

- 2 IPCC (2022) Summary for policymakers. In Global Warming of 1,5°C: IPCC Special Report on Impacts of Global Warming of 1,5°C above Pre-Industrial Levels in Context of Strengthening Response to Climate Change, Sustainable Development, and Efforts to Eradicate Poverty. 1–24. Cambridge University Press, Cambridge.
- 3 Jørgensen LB, Ørsted M, Malte H, Wang T and Overgaard J (2022) Extreme escalation of heat failure rates in ectotherms with global warming. *Nature* **611**, 93–98.
- 4 Engeszer RE, Patterson LB, Rao AA and Parichy DM (2007) Zebrafish in the wild: a review of natural history and new notes from the field. *Zebrafish* **4**, 21–40.
- 5 Dahms H-U and Lee J-S (2010) UV radiation in marine ectotherms: molecular effects and responses. *Aquat Toxicol* **97**, 3–14.
- 6 Feugere L, Angell L, Fagents J, Nightingale R, Rowland K, Skinner S, Hardege J, Bartels-Hardege H and Wollenberg Valero KC (2021) Behavioural stress propagation in benthic invertebrates caused by acute pH drop-induced metabolites. *Front Mar Sci* **8**, 870.
- 7 Feugere L, Scott VF, Rodriguez-Barucg Q, Beltran-Alvarez P and Wollenberg Valero KC (2021) Thermal stress induces a positive phenotypic and molecular feedback loop in zebrafish embryos. *J Therm Biol* **102**, 103114.
- 8 Halpern BS, Frazier M, Potapenko J, Casey KS, Koenig K, Longo C, Lowndes JS, Rockwood RC, Selig ER, Selkoe KA et al. (2015) Spatial and temporal changes in cumulative human impacts on the world's ocean. *Nat Commun* **6**, 7615.
- 9 Piggott JJ, Townsend CR and Matthaei CD (2015) Reconceptualizing synergism and antagonism among multiple stressors. *Ecol Evol* **5**, 1538–1547.
- 10 Rodgers EM and Gomez Isaza DF (2021) Harnessing the potential of cross-protection stressor interactions for conservation: a review. *Conserv Physiol* **9**, coab037.
- 11 Rodgers EM and Gomez Isaza DF (2023) The mechanistic basis and adaptive significance of cross-tolerance: a “pre-adaptation” to a changing world? *J Exp Biol* **226**, jeb245644.
- 12 Eleftheratos K, Kapsomenakis J, Fountoulakis I, Zerefos CS, Jöckel P, Dameris M, Bais AF, Bernhard G, Kouklaki D, Tourpali K et al. (2022) Ozone, DNA-active UV radiation, and cloud changes for the near-global mean and at high latitudes due to enhanced greenhouse gas concentrations. *Atmos Chem Phys* **22**, 12827–12855.
- 13 Downie AT, Wu NC, Cramp RL and Franklin CE (2023) Sublethal consequences of ultraviolet radiation exposure on vertebrates: synthesis through meta-analysis. *Glob Chang Biol* **29**, 6620–6634.
- 14 Alves RN and Agustí S (2020) Effect of ultraviolet radiation (UVR) on the life stages of fish. *Rev Fish Biol Fish* **30**, 335–372.
- 15 Hird C, Lundsgaard NU, Downie AT, Cramp RL and Franklin CE (2024) Considering ultraviolet radiation in experimental biology: a neglected pervasive stressor. *J Exp Biol* **227**, jeb247231.
- 16 Peng S, Liao H, Zhou T and Peng S (2017) Effects of UVB radiation on freshwater biota: a meta-analysis: UVB radiation and freshwater biota. *Glob Ecol Biogeogr* **26**, 500–510.
- 17 Dahlke F, Lucassen M, Bickmeyer U, Wohlrab S, Puvanendran V, Mortensen A, Chierici M, Pörtner H-O and Storch D (2020) Fish embryo vulnerability to combined acidification and warming coincides with a low capacity for homeostatic regulation. *J Exp Biol* **223**, jeb212589.
- 18 Dahlke F, Wohlrab S, Butzin M and Pörtner H-O (2020) Thermal bottlenecks in the life cycle define climate vulnerability of fish. *Science* **369**, 65–70.
- 19 Lundsgaard NU, Cramp RL and Franklin CE (2022) Early exposure to UV radiation causes telomere shortening and poorer condition later in life. *J Exp Biol* **225**, jeb243924.
- 20 Ceccato E, Cramp RL, Seebacher F and Franklin CE (2016) Early exposure to ultraviolet-B radiation decreases immune function later in life. *Conserv Physiol* **4**, cow037.
- 21 Cramp RL, Reid S, Seebacher F and Franklin CE (2014) Synergistic interaction between UVB radiation and temperature increases susceptibility to parasitic infection in a fish. *Biol Lett* **10**, 20140449.
- 22 Icoğlu Aksakal F and Ciltas A (2018) The impact of ultraviolet B (UV-B) radiation in combination with different temperatures in the early life stage of zebrafish (*Danio rerio*). *Photochem Photobiol Sci* **17**, 35–41.
- 23 Lupu A, Pechkovskaya A, Rashkovetsky E, Nevo E and Korol A (2004) DNA repair efficiency and thermotolerance in *Drosophila melanogaster* from “evolution canyon”. *Mutagenesis* **19**, 383–390.
- 24 Alton LA and Franklin CE (2012) Do high temperatures enhance the negative effects of ultraviolet-B radiation in embryonic and larval amphibians? *Biol Open* **1**, 897–903.
- 25 Berger D, Stångberg J, Grieshop K, Martinossi-Allibert I and Arnqvist G (2017) Temperature effects on life-history trade-offs, germline maintenance and mutation rate under simulated climate warming. *Proc Biol Sci* **284**, 20171721.
- 26 O'Connor CM, Gilmour KM, Arlinghaus R, Hasler CT, Philipp DP and Cooke SJ (2010) Seasonal carryover effects following the administration of cortisol to a wild teleost fish. *Physiol Biochem Zool* **83**, 950–957.

- 27 O'Connor CM, Norris DR, Crossin GT and Cooke SJ (2014) Biological carryover effects: linking common concepts and mechanisms in ecology and evolution. *Ecosphere* **5**, 1–11.
- 28 Lundsgaard NU, Hird C, Doody KA, Franklin CE and Cramp RL (2023) Carryover effects from environmental change in early life: an overlooked driver of the amphibian extinction crisis? *Glob Chang Biol* **29**, 3857–3868.
- 29 Todgham AE and Stillman JH (2013) Physiological responses to shifts in multiple environmental stressors: relevance in a changing world. *Integr Comp Biol* **53**, 539–544.
- 30 Hird C, Cramp RL and Franklin CE (2023) Thermal compensation reduces DNA damage from UV radiation. *J Therm Biol* **117**, 103711.
- 31 Rastogi RP, Richa, Kumar A, Tyagi MB and Sinha RP (2010) Molecular mechanisms of ultraviolet radiation-induced DNA damage and repair. *J Nucleic Acids* **2010**, 592980.
- 32 Dong Q, Todd Monroe W, Tiersch TR and Svoboda KR (2008) UVA-induced photo recovery during early zebrafish embryogenesis. *J Photochem Photobiol B* **93**, 162–171.
- 33 Banaś AK, Zgłobicki P, Kowalska E, Bažant A, Dziga D and Strzałka W (2020) All you need is light. Photorepair of UV-induced pyrimidine dimers. *Genes (Basel)* **11**, 1304.
- 34 Griffiths HR, Mistry P, Herbert KE and Lunec J (1998) Molecular and cellular effects of ultraviolet light-induced genotoxicity. *Crit Rev Clin Lab Sci* **35**, 189–237.
- 35 Jiricny J (2013) Postreplicative mismatch repair. *Cold Spring Harb Perspect Biol* **5**, a012633.
- 36 Minten EV and Yu DS (2019) DNA repair: translation to the clinic. *Clin Oncol* **31**, 303–310.
- 37 Salo HM, Jokinen EI, Markkula SE, Aaltonen TM and Penttilä HT (2000) Comparative effects of UVA and UVB irradiation on the immune system of fish. *J Photochem Photobiol B* **56**, 154–162.
- 38 Hurem S, Fraser TWK, Gomes T, Mayer I and Christensen T (2018) Sub-lethal UV radiation during early life stages alters the behaviour, heart rate and oxidative stress parameters in zebrafish (*Danio rerio*). *Ecotoxicol Environ Saf* **166**, 359–365.
- 39 Reardon RM, Walsh AK, Larsen CI, Schmidberger LH, Morrow LA, Thompson AE, Wellik IM and Thompson JS (2022) An epigenetically inherited UV hyper-resistance phenotype in *Saccharomyces cerevisiae*. *Epigenetics Chromatin* **15**, 31.
- 40 Shen Y, Stanislaukas M, Li G, Zheng D and Liu L (2017) Epigenetic and genetic dissections of UV-induced global gene dysregulation in skin cells through multi-omics analyses. *Sci Rep* **7**, 42646.
- 41 Dong Q, Svoboda K, Tiersch TR and Monroe WT (2007) Photobiological effects of UVA and UVB light in zebrafish embryos: evidence for a competent photorepair system. *J Photochem Photobiol B* **88**, 137–146.
- 42 Sussman R (2007) DNA repair capacity of zebrafish. *Proc Natl Acad Sci U S A* **104**, 13379–13383.
- 43 Pei D-S and Strauss PR (2013) Zebrafish as a model system to study DNA damage and repair. *Mutat Res* **743–744**, 151–159.
- 44 Feugere L, Bates A, Emagbetere T, Chapman E, Malcolm LE, Bulmer K, Hardege J, Beltran-Alvarez P and Wollenberg Valero KC (2023) Heat induces multiomic and phenotypic stress propagation in zebrafish embryos. *PNAS Nexus* **2**, gad137.
- 45 Trautinger F, Kindäs-Mügge I, Knobler RM and Hönigsmann H (1996) Stress proteins in the cellular response to ultraviolet radiation. *J Photochem Photobiol B* **35**, 141–148.
- 46 Liu J, Liu L, He J, Xu Y and Wang Y (2021) Multi-omic analysis of altered transcriptome and epigenetic signatures in the UV-induced DNA damage response. *DNA Repair (Amst)* **106**, 103172.
- 47 Boudoures AL, Pfeil JJ, Steenkiste EM, Hoffman RA, Bailey EA, Wilkes SE, Higdon SK and Thompson JS (2017) A novel histone crosstalk pathway important for regulation of UV-induced DNA damage repair in *Saccharomyces cerevisiae*. *Genetics* **206**, 1389–1402.
- 48 Berens JT and Molinier J (2020) Formation and recognition of UV-induced DNA damage within genome complexity. *Int J Mol Sci* **21**, 6689.
- 49 Cold Spring Harbor Laboratory Press (2011) E3 medium (for zebrafish embryos). Cold spring Harb Protoc 2011, db.rec66449.
- 50 Kimmel CB, Ballard WW, Kimmel SR, Ullmann B and Schilling TF (1995) Stages of embryonic development of the zebrafish. *Dev Dyn* **203**, 253–310.
- 51 Chrousos GP (1998) Stressors, stress, and neuroendocrine integration of the adaptive response. The 1997 Hans Selye memorial lecture. *Ann N Y Acad Sci* **851**, 311–335.
- 52 Barton BA (2002) Stress in fishes: a diversity of responses with particular reference to changes in circulating corticosteroids. *Integr Comp Biol* **42**, 517–525.
- 53 Barton BA and Iwama GK (1991) Physiological changes in fish from stress in aquaculture with emphasis on the response and effects of corticosteroids. *Annu Rev Fish Dis* **1**, 3–26.
- 54 Chrousos GP (2009) Stress and disorders of the stress system. *Nat Rev Endocrinol* **5**, 374–381.
- 55 Steindal IAF and Whitmore D (2020) Zebrafish circadian clock entrainment and the importance of broad spectral light sensitivity. *Front Physiol* **11**, 1002.
- 56 Takele Assefa A, Vandesompele J and Thas O (2020) On the utility of RNA sample pooling to optimize cost

- and statistical power in RNA sequencing experiments. *BMC Genomics* **21**, 312.
- 57 Chen S, Zhou Y, Chen Y and Gu J (2018) Fastp: an ultra-fast all-in-one FASTQ preprocessor. *Bioinformatics* **34**, i884–i890.
- 58 Sayols S, Scherzinger D and Klein H (2016) dupRadar: a Bioconductor package for the assessment of PCR artifacts in RNA-Seq data. *BMC Bioinformatics* **17**, 428.
- 59 Dobin A, Davis CA, Schlesinger F, Drenkow J, Zaleski C, Jha S, Batut P, Chaisson M and Gingeras TR (2013) STAR: ultrafast universal RNA-seq aligner. *Bioinformatics* **29**, 15–21.
- 60 Love MI, Huber W and Anders S (2014) Moderated estimation of fold change and dispersion for RNA-seq data with DESeq2. *Genome Biol* **15**, 550.
- 61 R Core Team (2020) R: A Language and Environment for Statistical Computing. R Foundation for Statistical Computing, Vienna.
- 62 Morgan M (2021) BiocManager: Access the Bioconductor Project Package Repository.
- 63 Duda JC, Drenda C, Kästel H, Rahnenführer J and Kappenberg F (2023) Benefit of using interaction effects for the analysis of high-dimensional time-response or dose-response data for two-group comparisons. *Sci Rep* **13**, 20804.
- 64 Love MI, Anders S and Huber W (2025) Analyzing RNA-seq data with DESeq2.
- 65 Blighe K, Rana S and Lewis M (2020) EnhancedVolcano: Publication-ready volcano plots with enhanced colouring and labeling.
- 66 Durinck S, Moreau Y, Kasprzyk A, Davis S, De Moor B, Brazma A and Huber W (2005) BioMart and Bioconductor: a powerful link between biological databases and microarray data analysis. *Bioinformatics* **21**, 3439–3440.
- 67 Durinck S, Spellman PT, Birney E and Huber W (2009) Mapping identifiers for the integration of genomic datasets with the R/Bioconductor package biomaRt. *Nat Protoc* **4**, 1184–1191.
- 68 Alexa A and Rahnenführer J (2020) topGO: Enrichment Analysis for Gene Ontology.
- 69 Carlson M (2020) org.Dr.eb: Genome wide annotation for Zebrafish.
- 70 Falcon S and Gentleman R (2007) Using GOstats to test gene lists for GO term association. *Bioinformatics* **23**, 257–258.
- 71 Yu G, Wang L-G, Han Y and He Q-Y (2012) clusterProfiler: an R package for comparing biological themes among gene clusters. *Omics* **16**, 284–287.
- 72 Yu G and He Q-Y (2016) ReactomePA: an R/Bioconductor package for reactome pathway analysis and visualization. *Mol Biosyst* **12**, 477–479.
- 73 Wickham H (2016) ggplot2: Elegant Graphics for Data Analysis. Springer, New York, NY.
- 74 Kassambara A (2021) rstatix: Pipe-Friendly Framework for Basic Statistical Tests.
- 75 Kassambara A (2020) ggpubr: “ggplot2” Based Publication Ready Plots.
- 76 Lenth RV (2022) emmeans: Estimated Marginal Means, aka Least-Squares Means.
- 77 Peterson RA and Cavanaugh JE (2020) Ordered quantile normalization: a semiparametric transformation built for the cross-validation era. *J Appl Stat* **47**, 2312–2327.
- 78 Peterson R (2021) Finding optimal normalizing transformations via bestNormalize. *R J* **13**, 310.
- 79 Zeileis and Hothorn (2002) Diagnostic checking in regression relationships. *R News* **2**, 7–10.
- 80 Mangiafico S (2021) rcompanion: Functions to Support Extension Education Program Evaluation. R package version 1.
- 81 Wei T and Simko V (2021) R package “corrplot”: Visualization of a Correlation Matrix.
- 82 Oksanen J, Blanchet FG, Friendly M, Kindt R, Legendre P, McGlenn D, Minchin PR, O’Hara RB, Simpson GL, Solymos P *et al.* (2020) vegan: Community Ecology Package.
- 83 Martinez Arbizu P (2017) pairwiseAdonis: Pairwise Multilevel Comparison using Adonis.
- 84 Vu VQ (2011) ggbiplot: A ggplot2 based biplot.
- 85 Lüdtke D (2021) Data Visualization for Statistics in Social Science. R package sjPlot version 2.8.7.
- 86 Muff S, Nilsen EB, O’Hara RB and Nater CR (2022) Rewriting results sections in the language of evidence. *Trends Ecol Evol* **37**, 203–210.
- 87 Sawilowsky SS (2009) New effect size rules of thumb. *J Mod Appl Stat Methods* **8**, 26.
- 88 Feugere L, De Silva Freitas C, Bates A, Storey K, Beltran-Alvarez P and Wollenberg Valero KC (2025) Data for: Social context prevents heat hormetic effects against mutagens during fish development [Data set].
- 89 Leung JYS and McAfee D (2020) Stress across life stages: impacts, responses and consequences for marine organisms. *Sci Total Environ* **700**, 134491.
- 90 Whitehouse LM, McDougall CS, Stefanovic DI, Boreham DR, Somers CM, Wilson JY and Manzoni RG (2017) Development of the embryonic heat shock response and the impact of repeated thermal stress in early stage lake whitefish (*Coregonus clupeaformis*) embryos. *J Therm Biol* **69**, 294–301.
- 91 Vindas MA, Fokos S, Pavlidis M, Höglund E, Dionysopoulou S, Ebbesson LOE, Papandroulakis N and Dermon CR (2018) Early life stress induces long-term changes in limbic areas of a teleost fish: the role of catecholamine systems in stress coping. *Sci Rep* **8**, 5638.
- 92 Donelan SC, Breitburg D and Ogburn MB (2021) Context-dependent carryover effects of hypoxia and

- warming in a coastal ecosystem engineer. *Ecol Appl* **31**, e02315.
- 93 Iordanov MS, Pribnow D, Magun JL, Dinh TH, Pearson JA and Magun BE (1998) Ultraviolet radiation triggers the ribotoxic stress response in mammalian cells. *J Biol Chem* **273**, 15794–15803.
- 94 Bianchi M, Giacomini E, Crinelli R, Radici L, Carloni E and Magnani M (2015) Dynamic transcription of ubiquitin genes under basal and stressful conditions and new insights into the multiple UBC transcript variants. *Gene* **573**, 100–109.
- 95 Simon MM, Reikerstorfer A, Schwarz A, Krone C, Luger TA, Jäättelä M and Schwarz T (1995) Heat shock protein 70 overexpression affects the response to ultraviolet light in murine fibroblasts. Evidence for increased cell viability and suppression of cytokine release. *J Clin Invest* **95**, 926–933.
- 96 Kowal P, Gurtan AM, Stuckert P, D'Andrea AD and Ellenberger T (2007) Structural determinants of human FANCF protein that function in the assembly of a DNA damage signaling complex. *J Biol Chem* **282**, 2047–2055.
- 97 Grompe M and D'Andrea A (2001) Fanconi anemia and DNA repair. *Hum Mol Genet* **10**, 2253–2259.
- 98 Yao C, Du W, Chen H, Xiao S, Huang L and Chen F-P (2015) Involvement of Fanconi anemia genes FANCD2 and FANCF in the molecular basis of drug resistance in leukemia. *Mol Med Rep* **11**, 4605–4610.
- 99 Zhou JJ, Huang Y, Zhang X, Cheng Y, Tang L and Ma X (2017) Eyes absent gene (EYA1) is a pathogenic driver and a therapeutic target for melanoma. *Oncotarget* **8**, 105081–105092.
- 100 Farrell AW, Halliday GM and Lyons JG (2011) Chromatin structure following UV-induced DNA damage-repair or death? *Int J Mol Sci* **12**, 8063–8085.
- 101 Cook PJ, Ju BG, Telese F, Wang X, Glass CK and Rosenfeld MG (2009) Tyrosine dephosphorylation of H2AX modulates apoptosis and survival decisions. *Nature* **458**, 591–596.
- 102 Sample A and He Y-Y (2017) Autophagy in UV damage response. *Photochem Photobiol* **93**, 943–955.
- 103 Charron RA, Fenwick JC, Lean DR and Moon TW (2000) Ultraviolet-B radiation effects on antioxidant status and survival in the zebrafish, *Brachydanio rerio*. *Photochem Photobiol* **72**, 327–333.
- 104 Costantini D, Metcalfe NB and Monaghan P (2010) Ecological processes in a hormetic framework. *Ecol Lett* **13**, 1435–1447.
- 105 Calabrese EJ and Baldwin LA (2002) Defining hormesis. *Hum Exp Toxicol* **21**, 91–97.
- 106 Krauss J, Geiger-Rudolph S, Koch I, Nüsslein-Volhard C and Irion U (2014) A dominant mutation in tyrp1A leads to melanophore death in zebrafish. *Pigment Cell Melanoma Res* **27**, 827–830.
- 107 Braasch I, Liedtke D, Volf J-N and Scharl M (2009) Pigmentary function and evolution of tyrp1 gene duplicates in fish. *Pigment Cell Melanoma Res* **22**, 839–850.
- 108 Brenner M and Hearing VJ (2008) The protective role of melanin against UV damage in human skin. *Photochem Photobiol* **84**, 539–549.
- 109 Sant KE and Timme-Laragy AR (2018) Zebrafish as a model for toxicological perturbation of yolk and nutrition in the early embryo. *Curr Environ Health Rep* **5**, 125–133.
- 110 Reef R, Dunn S, Levy O, Dove S, Shemesh E, Brickner I, Leggat W and Hoegh-Guldberg O (2009) Photoreactivation is the main repair pathway for UV-induced DNA damage in coral planulae. *J Exp Biol* **212**, 2760–2766.
- 111 Groothuizen FS and Sixma TK (2016) The conserved molecular machinery in DNA mismatch repair enzyme structures. *DNA Repair* **38**, 14–23.
- 112 Oliveira MF, Geihs MA, França TFA, Moreira DC and Hermes-Lima M (2018) Is “preparation for oxidative stress” a case of physiological conditioning Hormesis? *Front Physiol* **9**, 945.
- 113 Costantini D, Monaghan P and Metcalfe NB (2012) Early life experience primes resistance to oxidative stress. *J Exp Biol* **215**, 2820–2826.
- 114 Giraud-Billoud M, Rivera-Ingraham GA, Moreira DC, Burmester T, Castro-Vazquez A, Carvajalino-Fernández JM, Dafre A, Niu C, Tremblay N, Paital B *et al.* (2019) Twenty years of the “preparation for oxidative stress” (POS) theory: Ecophysiological advantages and molecular strategies. *Comp Biochem Physiol A Mol Integr Physiol* **234**, 36–49.
- 115 Hayes JD and McLellan LI (1999) Glutathione and glutathione-dependent enzymes represent a co-ordinately regulated defence against oxidative stress. *Free Radic Res* **31**, 273–300.
- 116 Rattan SIS (2006) Hormetic modulation of aging and longevity by mild heat stress. *Dose Response* **3**, 533–546.
- 117 Jantschitsch C and Trautinger F (2003) Heat shock and UV-B-induced DNA damage and mutagenesis in skin. *Photochem Photobiol Sci* **2**, 899–903.
- 118 Sottile ML and Nadin SB (2018) Heat shock proteins and DNA repair mechanisms: an updated overview. *Cell Stress Chaperones* **23**, 303–315.
- 119 Sakai W, Yuasa-Sunagawa M, Kusakabe M, Kishimoto A, Matsui T, Kaneko Y, Akagi J-I, Huyghe N, Ikura M, Ikura T *et al.* (2020) Functional impacts of the ubiquitin-proteasome system on DNA damage recognition in global genome nucleotide excision repair. *Sci Rep* **10**, 19704.
- 120 MacFadyen EJ, Williamson CE, Grad G, Lowery M, Jeffrey WH and Mitchell DL (2004) Molecular response to climate change: temperature dependence of

- UV-induced DNA damage and repair in the freshwater crustacean *Daphnia pulex*. *Glob Chang Biol* **10**, 408–416.
- 121 Morison SA, Cramp RL, Alton LA and Franklin CE (2020) Cooler temperatures slow the repair of DNA damage in tadpoles exposed to ultraviolet radiation: implications for amphibian declines at high altitude. *Glob Chang Biol* **26**, 1225–1234.
- 122 Chien L-C, Wu Y-H, Ho T-N, Huang Y-Y and Hsu T (2020) Heat stress modulates nucleotide excision repair capacity in zebrafish (*Danio rerio*) early and mid-early embryos via distinct mechanisms. *Chemosphere* **238**, 124653.
- 123 Tamai TK, Vardhanabhuti V, Foulkes NS and Whitmore D (2004) Early embryonic light detection improves survival. *Curr Biol* **14**, R104–R105.
- 124 Hirayama J, Miyamura N, Uchida Y, Asaoka Y, Honda R, Sawanobori K, Todo T, Yamamoto T, Sassone-Corsi P and Nishina H (2009) Common light signaling pathways controlling DNA repair and circadian clock entrainment in zebrafish. *Cell Cycle* **8**, 2794–2801.
- 125 Weger BD, Sahinbas M, Otto GW, Mracek P, Armant O, Dolle D, Lahiri K, Vallone D, Ettwiller L, Geisler R *et al.* (2011) The light responsive transcriptome of the zebrafish: function and regulation. *PLoS One* **6**, e17080.
- 126 Ghosh SG, Becker K, Huang H, Dixon-Salazar T, Chai G, Salpietro V, Al-Gazali L, Waisfisz Q, Wang H, Vaux KK *et al.* (2018) Biallelic mutations in ADPRHL2, encoding ADP-Ribosylhydrolase 3, lead to a degenerative Pediatric stress-induced epileptic ataxia syndrome. *Am J Hum Genet* **103**, 431–439.
- 127 Zaksauskaite R, Thomas RC, van Eeden F and El-Khamisy SF (2021) Tdp1 protects from topoisomerase I-mediated chromosomal breaks in adult zebrafish but is dispensable during larval development. *Sci Adv* **7**, eabc4165.
- 128 Lanza A, Tornaletti S, Rodolfo C, Scanavini MC and Pedrini AM (1996) Human DNA topoisomerase I-mediated cleavages stimulated by ultraviolet light-induced DNA damage (\*). *J Biol Chem* **271**, 6978–6986.
- 129 Subramanian D, Rosenstein BS and Muller MT (1998) Ultraviolet-induced DNA damage stimulates topoisomerase I-DNA complex formation in vivo: possible relationship with DNA repair. *Cancer Res* **58**, 976–984.
- 130 Goellner EM, Putnam CD and Kolodner RD (2015) Exonuclease I-dependent and independent mismatch repair. *DNA Repair* **32**, 24–32.
- 131 Das L, Quintana VG and Sweasy JB (2020) NTHL1 in genomic integrity, aging and cancer. *DNA Repair* **93**, 102920.
- 132 Chen Z, Gan J, Wei Z, Zhang M, Du Y, Xu C and Zhao H (2022) The emerging role of PRMT6 in cancer. *Front Oncol* **12**, 841381.
- 133 El-Andaloussi N, Valovka T, Toueille M, Steinacher R, Focke F, Gehrig P, Covic M, Hassa PO, Schär P, Hübscher U *et al.* (2006) Arginine methylation regulates DNA polymerase beta. *Mol Cell* **22**, 51–62.
- 134 Zhao X-X, Zhang Y-B, Ni P-L, Wu Z-L, Yan Y-C and Li Y-P (2016) Protein arginine Methyltransferase 6 (Prmt6) is essential for early zebrafish development through the direct suppression of gadd45 $\alpha$  stress sensor gene. *J Biol Chem* **291**, 402–412.
- 135 Xu D, Guo R, Sobock A, Bachrati CZ, Yang J, Enomoto T, Brown GW, Hoatlin ME, Hickson ID and Wang W (2008) RMI, a new OB-fold complex essential for bloom syndrome protein to maintain genome stability. *Genes Dev* **22**, 2843–2855.
- 136 Patel DS, Misenko SM, Her J and Bunting SF (2017) BLM helicase regulates DNA repair by counteracting RAD51 loading at DNA double-strand break sites. *J Cell Biol* **216**, 3521–3534.
- 137 Hudson DF, Amor DJ, Boys A, Butler K, Williams L, Zhang T and Kalitsis P (2016) Loss of RMI2 increases genome instability and causes a bloom-like syndrome. *PLoS Genet* **12**, e1006483.
- 138 Brinkmann K, Schell M, Hoppe T and Kashkar H (2015) Regulation of the DNA damage response by ubiquitin conjugation. *Front Genet* **6**, 98.
- 139 Cukras S, Morffy N, Ohn T and Kee Y (2014) Inactivating UBE2M impacts the DNA damage response and genome integrity involving multiple cullin ligases. *PLoS One* **9**, e101844.
- 140 Stewart MD, Ritterhoff T, Klevit RE and Brzovic PS (2016) E2 enzymes: more than just middle men. *Cell Res* **26**, 423–440.
- 141 Hanakahi LA, Bartlett-Jones M, Chappell C, Pappin D and West SC (2000) Binding of inositol phosphate to DNA-PK and stimulation of double-strand break repair. *Cell* **102**, 721–729.
- 142 Wan Q-L, Meng X, Dai W, Luo Z, Wang C, Fu X, Yang J, Ye Q and Zhou Q (2021) N<sup>6</sup>-methyldeoxyadenine and histone methylation mediate transgenerational survival advantages induced by hormetic heat stress. *Sci Adv* **7**, eabc3026.
- 143 Haarmann-Stemmann T, Boege F and Krutmann J (2013) Adaptive and maladaptive responses in skin: mild heat exposure protects against UVB-induced photoaging in mice. *J Invest Dermatol* **133**, 868–871.
- 144 Higginson AD (2020) Identifying reliable fitness proxies for growing animals responding to anthropogenic changes. *bioRxiv*. [10.1101/2020.08.06.239616](https://doi.org/10.1101/2020.08.06.239616)
- 145 Cocciardi JM, O'Brien EK, Hoskin CJ, Stoetzel H and Higgie M (2021) The predictive potential of key adaptation parameters and proxy fitness traits between

- benign and stressful thermal environments. *bioRxiv*. [10.1101/2021.04.29.441345](https://doi.org/10.1101/2021.04.29.441345)
- 146 Lind J and Cresswell W (2005) Determining the fitness consequences of antipredation behavior. *Behav Ecol* **16**, 945–956.
- 147 Morgan R, Andreassen AH, Åsheim ER, Finnøen MH, Dresler G, Brembu T, Loh A, Miest JJ and Jutfelt F (2022) Reduced physiological plasticity in a fish adapted to stable temperatures. *Proc Natl Acad Sci U S A* **119**, e2201919119.
- 148 Matsuda M, Hoshino T, Yamakawa N, Tahara K, Adachi H, Sobue G, Maji D, Ihn H and Mizushima T (2013) Suppression of UV-induced wrinkle formation by induction of HSP70 expression in mice. *J Invest Dermatol* **133**, 919–928.
- 149 Mathuru AS (2016) Conspecific injury raises an alarm in medaka. *Sci Rep* **6**, 36615.
- 150 Frisch K (1938) Zur Psychologie des Fisch-Schwarmes. *Naturwissenschaften* **26**, 601–606.
- 151 Crane AL, Bairos-Novak KR, Goldman JA and Brown GE (2022) Chemical disturbance cues in aquatic systems: a review and prospectus. *Ecological monographs* **92**, e01487.
- 152 Fortier S, Yang X, Wang Y, Bennett RAO and Strauss PR (2009) Base excision repair in early zebrafish development: evidence for DNA polymerase switching and standby AP endonuclease activity. *Biochemistry* **48**, 5396–5404.
- 153 Wu X and Hammer JA (2014) Melanosome transfer: it is best to give and receive. *Curr Opin Cell Biol* **29**, 1–7.
- 154 Wondrak GT, Jacobson MK and Jacobson EL (2006) Endogenous UVA-photosensitizers: mediators of skin photodamage and novel targets for skin photoprotection. *Photochem Photobiol Sci* **5**, 215–237.
- 155 Nair RR, Hsu J, Jacob JT, Pineda CM, Hobbs RP and Coulombe PA (2021) A role for keratin 17 during DNA damage response and tumor initiation. *Proc Natl Acad Sci U S A* **118**, e2020150118.
- 156 Elsakrmy N, Aouida M, Hindi N, Moovarkumudalvan B, Mohanty A, Ali R and Ramotar D (2022) *C. elegans* ribosomal protein S3 protects against H<sub>2</sub>O<sub>2</sub>-induced DNA damage and suppresses spontaneous mutations in yeast. *DNA Repair* **117**, 103359.
- 157 Bridge WL, Vandenberg CJ, Franklin RJ and Hiom K (2005) The BRIP1 helicase functions independently of BRCA1 in the Fanconi anemia pathway for DNA crosslink repair. *Nat Genet* **37**, 953–957.
- 158 Gibney ER and Nolan CM (2010) Epigenetics and gene expression. *Heredity* **105**, 4–13.
- 159 Bui D-C, Kim J-E, Shin J, Lim JY, Choi GJ, Lee Y-W, Seo J-A and Son H (2019) ARS2 plays diverse roles in DNA damage response, fungal development, and pathogenesis in the plant pathogenic fungus *Fusarium graminearum*. *Front Microbiol* **10**, 2326.
- 160 Rossman TG and Wang Z (1999) Expression cloning for arsenite-resistance resulted in isolation of tumor-suppressor *fauc* cDNA: possible involvement of the ubiquitin system in arsenic carcinogenesis. *Carcinogenesis* **20**, 311–316.
- 161 Vougiouklakis T, Bernard BJ, Nigam N, Burkitt K, Nakamura Y and Saloura V (2020) Clinicopathologic significance of protein lysine methyltransferases in cancer. *Clin Epigenetics* **12**, 146.
- 162 Albig W, Meergans T and Doenecke D (1997) Characterization of the H1.5 gene completes the set of human H1 subtype genes. *Gene* **184**, 141–148.
- 163 Li H, Zhong Y, Wang Z, Gao J, Xu J, Chu W, Zhang J, Fang S and Du SJ (2013) Smyd1b is required for skeletal and cardiac muscle function in zebrafish. *Mol Biol Cell* **24**, 3511–3521.
- 164 Tan X, Rotllant J, Li H, De yne P and Du SJ (2006) SmyD1, a histone methyltransferase, is required for myofibril organization and muscle contraction in zebrafish embryos. *Proc Natl Acad Sci U S A* **103**, 2713–2718.
- 165 Jackson MC, Loewen CJG, Vinebrooke RD and Chimimba CT (2016) Net effects of multiple stressors in freshwater ecosystems: a meta-analysis. *Glob Chang Biol* **22**, 180–189.
- 166 Sessions KJ, Whitehouse LM, Manzon LA, Boreham DR, Somers CM, Wilson JY and Manzon RG (2021) The heat shock response shows plasticity in embryonic lake whitefish (*Coregonus clupeaformis*) exposed to repeated thermal stress. *J Therm Biol* **100**, 103036.
- 167 Villamizar N, Vera LM, Foulkes NS and Sánchez-Vázquez FJ (2014) Effect of lighting conditions on zebrafish growth and development. *Zebrafish* **11**, 173–181.
- 168 Bais AF, Lucas RM, Bornman JF, Williamson CE, Sulzberger B, Austin AT, Wilson SR, Andrady AL, Bernhard G, McKenzie RL *et al.* (2018) Environmental effects of ozone depletion, UV radiation and interactions with climate change: UNEP environmental effects assessment panel, update 2017. *Photochem Photobiol Sci* **17**, 127–179.
- 169 Ficke AD, Myrick CA and Hansen LJ (2007) Potential impacts of global climate change on freshwater fisheries. *Rev Fish Biol Fish* **17**, 581–613.

## Supporting information

Additional supporting information may be found online in the Supporting Information section at the end of the article.

**Dataset S1.** For ‘Social context prevents heat hormetic effects against mutagens during fish development’. Dataset providing the statistical tests and the

functional enrichment of differentially expressed genes as detected by DESeq2.

**Dataset S2.** For ‘Social context prevents heat hormetic effects against mutagens during fish development’. Dataset providing the list of genes and their log-2-fold-change and *P*-values (raw and adjusted) calculated using two different models: limma-voom and DESeq2.

**Fig. S1.** The transcriptomic response to UVR has common and unique components depending on heat stress history.

**Fig. S2.** Heat stress history treatments altered the normal transcriptomic response to ultraviolet radiation.

**Fig. S3.** Social metabolites impaired behaviour whilst heat tended to facilitate swimming through better repair.

**Data S1.** Supplementary methods.